

AD-A219 257

DTIC FILE COPY

2

NAVAL POSTGRADUATE SCHOOL Monterey, California



THESIS

AN APPROACH FOR DESIGN AND ANALYSIS OF
COMPOSITE ROTOR BLADES

by

Geraldo A. Macedo Moura

September 1989

Thesis Advisor:

Ramesh Kolar

Approved for public release; distribution is unlimited.

DTIC
ELECTE
MAR 16 1990
S B D

90 03 16 0614

UNCLASSIFIED

SECURITY CLASSIFICATION OF THIS PAGE

REPORT DOCUMENTATION PAGE

1a REPORT SECURITY CLASSIFICATION UNCLASSIFIED		1b RESTRICTIVE MARKINGS	
2a SECURITY CLASSIFICATION AUTHORITY		3 DISTRIBUTION/AVAILABILITY OF REPORT <i>Approved for public release; Distribution is unlimited.</i>	
2b DECLASSIFICATION/DOWNGRADING SCHEDULE		4 PERFORMING ORGANIZATION REPORT NUMBER(S)	
5 MONITORING ORGANIZATION REPORT NUMBER(S)		6a NAME OF PERFORMING ORGANIZATION Naval Postgraduate School	
7a NAME OF MONITORING ORGANIZATION Naval Postgraduate School		8b OFFICE SYMBOL (if applicable) 31	
6c ADDRESS (City, State, and ZIP Code) Monterey, CA 93943-5000		7b ADDRESS (City, State, and ZIP Code) Monterey, CA 93943-5000	
8a NAME OF FUNDING, SPONSORING ORGANIZATION		9 PROCUREMENT INSTRUMENT IDENTIFICATION NUMBER	
8b OFFICE SYMBOL (if applicable)		10 SOURCE OF FUNDING NUMBERS	
8c ADDRESS (City, State, and ZIP Code)		PROGRAM ELEMENT NO	PROJECT NO
		TASK NO	WORK UNIT ACCESSION NO
11 TITLE (Include Security Classification) An Approach for Design and Analysis of Composite Rotor Blades			
12 PERSONAL AUTHOR(S) Geraldo A. Macedo Moura			
13a TYPE OF REPORT Master's Thesis	13b TIME COVERED FROM TO	14 DATE OF REPORT (Year, Month, Day) September, 1989	15 PAGE COUNT 87
16 SUPPLEMENTARY NOTATION <i>The views expressed in this thesis are those of the author and do not reflect the official policy or position of the Department of Defense or U.S. Government.</i>			
COSATI CODES		17b SUBJECT TERMS (Continue on reverse if necessary and identify by block number)	
FIELD	GROUP	SUB-GROUP	
		Composite materials, Rotor Design, Extension-Twist couplings, Tilt-Rotor, Vibration, Assymmetric laminates. (EG)	
19 ABSTRACT (Continue on reverse if necessary and identify by block number) <i>The advent of tilt rotor technology asks for rotors that have different twist and RPM requirements in hover and in forward flight to optimize for operational conditions. In order to get an assessment of the capabilities to fulfill these requirements this report presents a mapping of twist angle variation as a function of RPM and laminate orientation. The basic laminate for the six models as well the D-shape spar that represents the structurally active part of the blade is assumed to be constant (0°/90°/0°/90°/90°/0°). This six layer cross ply laminate is chosen as it provides the necessary extension-twist coupling without a hygrothermally induced twist that is highly undesirable. The couplings and trends in the models are visualized in carpet plots, one for each model, in an attempt to establish a method to answer the basic question of the magnitude of twist angle available due to a particular geometry, material and load system.</i>			
20 DISTRIBUTION/AVAILABILITY OF ABSTRACT <input checked="" type="checkbox"/> UNCLASSIFIED/UNLIMITED <input type="checkbox"/> SAME AS RPT <input type="checkbox"/> DTIC USERS		21 ABSTRACT SECURITY CLASSIFICATION UNCLASSIFIED	
22a NAME OF RESPONSIBLE INDIVIDUAL Ramesh Kolar		22b TELEPHONE (Include Area Code) (408) 646-2491/2938	22c OFFICE SYMBOL 67KJ

Approved for public release; distribution is unlimited.

An Approach for Design and Analysis
of Composite Rotor Blades

by

Geraldo A. Macedo Moura
Major Aviador, Força Aérea Brasileira
B.S., Instituto Tecnológico de Aeronáutica

Submitted in partial fulfillment
of the requirements for the degree of

MASTER OF SCIENCE IN AERONAUTICAL ENGINEERING

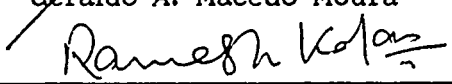
from the

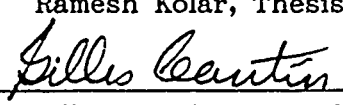
NAVAL POSTGRADUATE SCHOOL
September 1989

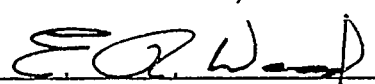
Author:


Geraldo A. Macedo Moura

Approved by:


Ramesh Kolar, Thesis Advisor


Gilles Cantin, Second Reader


E. Roberts Wood, Chairman
Department of Aeronautics and Astronautics

ABSTRACT

The advent of tilt rotor technology asks for rotors that have different twist and RPM requirements in hover and in forward flight to optimize for operational conditions. In order to get an assessment of the capabilities to fulfill these requirements this report presents a mapping of twist angle variation as a function of RPM and laminate orientation. The basic laminate for the six models as well the D-shape spar that represents the structurally active part of the blade is assumed to be constant ($0^\circ/90^\circ/0^\circ/90^\circ/90^\circ/0^\circ$). This six layer cross ply laminate is chosen as it provides the necessary extension-twist coupling without a hygrothermally induced twist that is highly undesirable. The couplings and trends in the models are visualized in carpet plots, one for each model, in an attempt to establish a method to answer the basic question of the magnitude of twist angle available due to a particular geometry, material and load system.

Accession For	
NTIS GRA&I	<input checked="checked" type="checkbox"/>
DTIC TAB	<input type="checkbox"/>
Unannounced	<input type="checkbox"/>
Justification	
By	
Distribution/	
Availability Codes	
Dist	Avail and/or Special
A-1	

TABLE OF CONTENTS

I. INTRODUCTION	1
A. OVERVIEW	1
B. LITERATURE REVIEW	2
C. THESIS OUTLINE	5
II. THEORETICAL FORMULATION	7
A. BASIC CONSIDERATIONS	7
B. STRESS-STRAIN RELATIONS	8
C. LAMINATE ANALYSIS	15
D. EFFECTS OF PLY ANGLE θ	20
III. ROTOR MODELING	27
A. TYPICAL CURRENT ROTOR MODELING	27
B. PROPOSED SOLUTION	27
C. GIFTS CAPABILITIES	29
D. VARIOUS ROTOR DESIGNS OR CONFIGURATIONS	34
IV. STATIC AND DYNAMIC ANALYSIS	39
A. TORSIONAL LOAD	39
B. LIFT AND BLADE WEIGHT LOADS	40
C. CENTRIFUGAL LOAD	42
D. MODAL ANALYSIS	50

V.	ANALYSIS OF RESULTS	52
A.	DYNAMIC BEHAVIOR	53
B.	STATIC BEHAVIOR	54
VI.	CONCLUSIONS AND SCOPE FOR FUTURE RESEARCH	60
A.	CONCLUSIONS	60
B.	SCOPE FOR FUTURE RESEARCH	61
	LIST OF REFERENCES	62
	BIBLIOGRAPHIC RESEARCH	66
ANNEX 1	- M120.SRC	72
ANNEX 2	- LAYUP.AUX	74
	INITIAL DISTRIBUTION LIST	79

ACKNOWLEDGEMENTS

I wish to dedicate this project to my wife, Angela, and my sons and daughter for their support and understanding during these two years in Monterey; also to my friend, Fernando, who, in 1982, directed my interests towards rotary-wing aircraft, saying that the future of aviation would be a faster vertical takeoff airplane.

I wish to thank my advisor, Professor Ramesh Kolar, for his help in completing this project, and his valuable corrections during the report writing. I would also like to thank Professor E.W. Wood for being always available to answer questions and Professor Gilles Cantin for his revision and comments.

I. INTRODUCTION

A. OVERVIEW

In the design process of composite material structures it is often noticed that the best characteristics of the material are not used. The normal procedure is to tailor the material to approach the properties of isotropic materials, avoiding the "undesirable" couplings between extension and twist for example.

That traditional approach worked for helicopter design. However, in the tilt rotor, the idea of changing the twist angle of the blade to optimize for either hover or forward flight came into the scenario.

This study will use a blade spar to study the sensitivity of the extension-twist coupling due to changes in RPM, layer angles definition, changes in laminate orientation and also the effects of each of these configurations in the first four natural vibration modes of the blade.

In the analysis, a program named CASA/GIFTS (Computer Aided Structural Analysis/Graphical Interactive Finite Element Total System) is adopted. The program makes it easier to visualize the effects of the coupling in the structure and is seen to be an efficient design tool. The results obtained through the finite element procedure for each laminate

configuration, in a total of six models will be presented in 3-D graphs that show the trends for each model for the layer angle (top layer as a reference), the RPM and the twist angle.

These graphs can then be used as a preliminary orientation by the designer to achieve the optimal or near optimal combination of laminate configuration layer angle within the laminate that fit the specific requirements for the particular blade in focus.

B. LITERATURE REVIEW

This section reviews briefly some pertinent publications listed as References in the thesis report. Other related literature found during the scope of this research, is listed under Bibliography. The topics reviewed are classified under the following categories:

- . Finite Element Theory.
- . Composite Material Theory.
- . Vibrations.
- . Helicopter Theory.
- . Design Applications (Modeling).
- . Auxiliary Software.

In the Finite Element Theory, relevant to present research, some basic references are: Batoz[1980] that describes the finite element procedures in engineering analysis using Discrete Kirchhoff Theory (DKT), Cook[1981] on

basic concepts and applications of finite element analysis, Craig[1981] describing computer methods in structural dynamics and [CASA/GIFTS, 1987] that is the reference manual for the finite element code used for the present (static and dynamic) work. Its graphical capabilities are very convenient to the analyst in a manner that simplifies the visualization of the effects of loads and couplings in the structure, making difficult concepts more accessible to understanding.

Tsai and Pagano[1968] establish a notation in which the composite lamina properties are invariant with respect to the axis of rotation. This approach provides a very useful way to compare various material systems; the laminate theory is well documented, see for example Vinson[1987] and Jones[1975] both offer a good source on the mechanics and behavior of composite materials.

Yntema[1955] developed a very useful tool to estimate bending frequencies of rotating beams in which the stiffness effect of RPM is shown for several blades (beam) configurations. Schilhansl[1958] uses another approach to estimate bending frequencies of rotating cantilever beams, introducing the effect of the angle made by the minor axis of inertia with the direction of the tangential circular velocity. Wood[1965] shows a parametric investigation of aerodynamic and aeroelastic characteristics of articulated and hingeless rotor systems. Pritchard[1988] presents an optimal placement of tuning masses to reduce vibration levels in

helicopter blades. Kottapalli[1983] approaches the vibration reduction problem by modifying the blade torsional response. This is an innovative approach in that he modifies the aerodynamic response instead of adding mass, which is the usual conventional way to solve the vibration reduction problem.

The helicopter theory in general is found comprehensively in Johnson[1980] and is complemented in this research by Prouty[1986] in the understanding design trends.

Hoskin[1986] is a general informative book in the aeronautical utilization of composite materials, and in Lake[1988] there is a preliminary investigation of finite element modeling of composite material rotor blades. Nixon[1987] addresses the extension-twist coupling of composite circular tubes applied to tilt rotor design. In McVeigh [1983] the aerodynamic design of XV-15 advanced composite tilt rotor blade requirements are reviewed. Finally Hodges[1987] presents a comparison of composite material rotor blade models, using two different methods of analysis: this model was chosen as a prime reference to build the basic model used throughout this work.

Several software tools made it possible to manipulate the immense volume of data transforming, it into a suitable and compact presentation form, enabling the conclusions to be obtained. Kelly[1988] was the basic reference to use Word Perfect 5.0 in the word processing and graphical editing jobs.

Holt[1988] is a reference that helps to manage the data into Lotus 1-2-3 files and to get the input graph files to Word Perfect and to SURFER[1987]. The SURFER program was used to obtain the 3-D carpet plots of extension-twist coupling analysis.

C. THESIS OUTLINE

This thesis report is divided into three areas, often found during a design process.

It begins by modeling a rotor blade with laminate composite material. A numerical solution is obtained, exploiting the extension-twist coupling inherent when asymmetries are present in the laminate construction. Discrepancies encountered in the results compared with other rotor models are reported. These differences raised questions fostering the research towards the possibilities of different rotor constructions, starting with the same basic laminate.

The different rotor configurations obtained are then subject to both static and dynamic analysis. The static analysis reveals the different responses of these models, while the dynamic behavior remains almost invariant, yielding only small variations in the first four fundamental vibration modes.

Analysis of the results is done, and it is believed that a new insight into finite element analysis of composite

laminates is provided. This new insight is better noticed when there are asymmetries present within the laminate construction.

II. THEORETICAL FORMULATION

A. BASIC CONSIDERATIONS

To understand how composite material works and its particular behavior that is useful in "designing" the material, a macroscopic approach is resorted to.

Composite means that two or more materials are combined and usually preserve their best qualities, and, often exhibit properties that neither one possesses by itself.

Some of the properties that can be improved by making a composite material are:

- . strength
- . stiffness
- . corrosion resistance
- . wear resistance
- . life in fatigue
- . thermal insulation
- . thermal conductivity
- . acoustical insulation

It may be noted that not all these properties are improved at the same time, and usually it may not be required.

An Orthotropic¹ material has properties which are different in three mutually perpendicular directions at a point, in other words has three different planes of symmetry.

A lamina is the basic form of any laminated fiber-reinforced composite, it consists of a plane mounting of fibers imbedded in a matrix.

In the macro-mechanical behavior of the lamina, only averaged apparent mechanical properties, or better, the stress-strain relations for an orthotropic material under plane stress conditions, transformed to directions not aligned with the principal directions of the lamina, are considered.

This describes the behavior of the orthotropic material whose laminae have arbitrary directions, other than the natural geometric directions of the structure to be analyzed.

B. STRESS-STRAIN RELATIONS

The stress-strain relations or generalized Hooke's law for anisotropic material will be reviewed briefly, and the basic restriction of linear elastic behavior assumption applies.

The following derivations can be found in more detail in Vinson[1987].

The elasticity tensor has nine independent elasticity constants, because of symmetry ($C_{ij}=C_{ji}$) and the three mutually

¹ - Orthogonally anisotropic.

orthogonal planes of symmetry ($C_{16}=C_{26}=C_{36}=C_{45}=0$);

that is,

$$(1) \quad C_{ij} = \begin{bmatrix} C_{11} & C_{12} & C_{13} & 0 & 0 & 0 \\ C_{21} & C_{22} & C_{23} & 0 & 0 & 0 \\ C_{31} & C_{32} & C_{33} & 0 & 0 & 0 \\ 0 & 0 & 0 & C_{44} & 0 & 0 \\ 0 & 0 & 0 & 0 & C_{55} & 0 \\ 0 & 0 & 0 & 0 & 0 & C_{66} \end{bmatrix}$$

and

$$(2) \quad \sigma_i = C_{ij} \times \epsilon_j \quad (i=1,2,3,4,5,6; j=1,2,3,4,5,6)^2$$

In these relations the hygrothermal and thermal effects are not included for the sake of simplicity of this report.

Through a force equilibrium study, analogous to the Mohr's circle analysis [Jones, 1975] the stresses and strains in the

²The material directions 1 to 6 are equivalent to cartesian directions: x,y,z,yz,xz,xy respectively in material axis.

material directions can be related to arbitrary³ directions using the following relations:

$$(3) \quad \begin{bmatrix} \sigma_x \\ \sigma_y \\ \sigma_z \\ \sigma_{yz} \\ \sigma_{xz} \\ \sigma_{xy} \end{bmatrix} = [T]^{-1} \begin{bmatrix} \sigma_1 \\ \sigma_2 \\ \sigma_3 \\ \sigma_4 \\ \sigma_5 \\ \sigma_6 \end{bmatrix}$$

and

$$(4) \quad \begin{bmatrix} \epsilon_x \\ \epsilon_y \\ \epsilon_z \\ \epsilon_{yz} \\ \epsilon_{xz} \\ \epsilon_{xy} \end{bmatrix} = [T]^{-1} \begin{bmatrix} \epsilon_1 \\ \epsilon_2 \\ \epsilon_3 \\ \epsilon_4 \\ \epsilon_5 \\ \epsilon_6 \end{bmatrix}$$

The transformation matrix is constructed by defining $m = \cos \theta$, $n = \sin \theta$; where θ is the ply orientation angle, defined with respect to material and structural axes, assuming positive sign in counterclockwise direction (Figure 1).

³ More convenient, xyz axis related to the structure geometry for example.

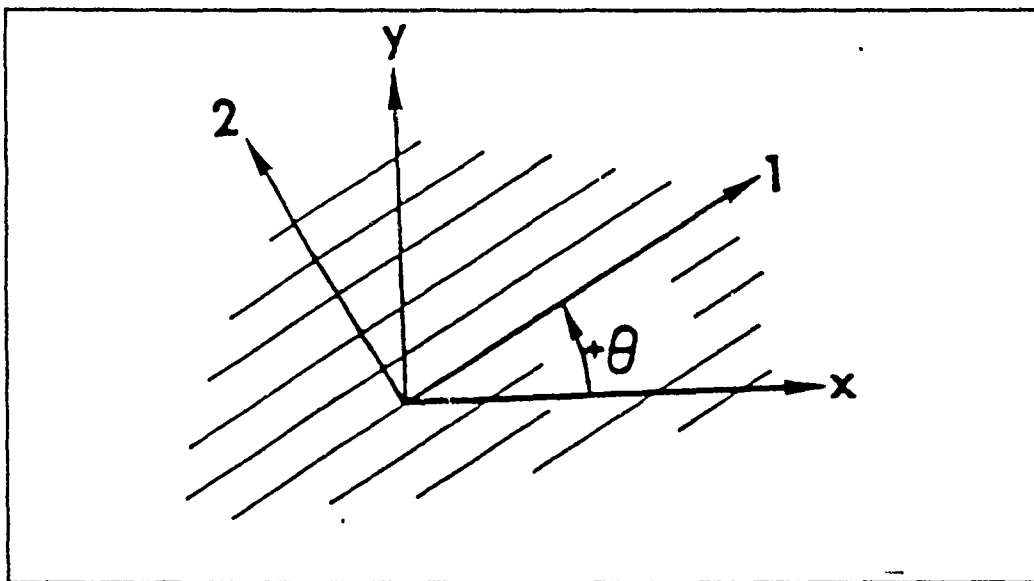


Figure 1 Positive rotation of principal material axes from arbitrary xy axes [Jones,1975].

The inverse of transformation matrix $[T]$ is expressed in terms of direction cosines m and n as:

$$(5) \quad [T]^{-1} = \begin{bmatrix} m^2 & n^2 & 0 & 0 & 0 & -2mn \\ n^2 & m^2 & 0 & 0 & 0 & +2mn \\ 0 & 0 & 1 & 0 & 0 & 0 \\ 0 & 0 & 0 & m & -n & 0 \\ 0 & 0 & 0 & n & m & 0 \\ -mn & 0 & 0 & 0 & 0 & (m^2 - n^2) \end{bmatrix}$$

For a lamina of composite material the modern notation uses Q_{ij} for the quantities in the material stiffness matrix and are defined as:

$$\begin{aligned}
 (6) \quad Q_{11} &= E_{11}(1 - \nu_{23}\nu_{32})/\delta, & Q_{22} &= E_{22}(1 - \nu_{31}\nu_{13})/\delta \\
 Q_{33} &= E_{33}(1 - \nu_{12}\nu_{21})/\delta, & Q_{44} &= G_{23}, & Q_{55} &= G_{13} \\
 Q_{12} &= E_{11}(\nu_{21} + \nu_{31}\nu_{23})/\delta = E_{22}(\nu_{12} + \nu_{32}\nu_{13})/\delta \\
 Q_{13} &= E_{11}(\nu_{31} + \nu_{21}\nu_{32})/\delta = E_{22}(\nu_{13} + \nu_{12}\nu_{23})/\delta \\
 Q_{23} &= E_{22}(\nu_{32} + \nu_{12}\nu_{31})/\delta = E_{33}(\nu_{23} + \nu_{21}\nu_{13})/\delta \\
 \delta &= 1 - \nu_{12}\nu_{21} - \nu_{23}\nu_{32} - \nu_{31}\nu_{13} - 2\nu_{21}\nu_{32}\nu_{13}
 \end{aligned}$$

If the lamina has same properties in both 2 and 3 directions, then $\nu_{12} = \nu_{13}$, $\nu_{31} = \nu_{32} = 0$, $G_{12} = G_{13}$, $E_{22} = E_{33}$ and a simplification in equations (6) lead to equations (7).

$$\begin{aligned}
 (7) \quad Q_{11} &= E_{11}/(1 - \nu_{12}\nu_{21}), & Q_{22} &= E_{22}/(1 - \nu_{12}\nu_{21}) \\
 Q_{12} &= \nu_{21}E_{11}/(1 - \nu_{12}\nu_{21}) = \nu_{12}E_{22}/(1 - \nu_{12}\nu_{21}) \\
 Q_{66} &= G_{12}
 \end{aligned}$$

To compare various material systems in the design of a composite structure, Tsai and Pagano[1969] arrived at some invariants with respect to the axis of rotation:

$$\begin{aligned}
 U_1 &= \frac{1}{8} (3Q_{11} + 3Q_{22} + 2Q_{12} + 4Q_{66}) \\
 U_2 &= \frac{1}{2} (Q_{11} - Q_{22}) \\
 (8) \quad U_3 &= \frac{1}{8} (Q_{11} + Q_{22} - 2Q_{12} - 4Q_{66}) \\
 U_4 &= \frac{1}{8} (Q_{11} + Q_{22} + 6Q_{12} - 4Q_{66}) \\
 U_5 &= \frac{1}{8} (Q_{11} + Q_{22} - 2Q_{12} + 4Q_{66})
 \end{aligned}$$

These invariants are representative of the lamina properties. The $[Q]$ matrix may be transformed to x-y axes from 1-2 axes by the usual coordinate transformation.

$$(9) \quad [\bar{Q}] = [T]^{-1} [Q][T]$$

In terms of the invariants U_s , the $[\bar{Q}]$ matrix elements are written as:

$$\begin{aligned}
 \bar{Q}_{11} &= U_1 + U_2 \cos(2\theta) + U_3 \cos(4\theta) \\
 \bar{Q}_{22} &= U_1 - U_2 \cos(2\theta) + U_3 \cos(4\theta) \\
 \bar{Q}_{12} &= U_4 - U_3 \cos(4\theta) \\
 (10) \quad \bar{Q}_{66} &= U_5 - U_3 \cos(4\theta) \\
 \bar{Q}_{16} &= \frac{1}{2} U_2 \sin(2\theta) + U_3 \sin(4\theta) \\
 \bar{Q}_{26} &= \frac{1}{2} U_2 \sin(2\theta) - U_3 \sin(4\theta)
 \end{aligned}$$

After the definitions in (10), the stress-strain relations for the k^{th} lamina of a N ply laminate (Figure 2) are given by:

$$(11) \quad \begin{bmatrix} \sigma_x \\ \sigma_y \\ \sigma_z \\ \sigma_{yz} \\ \sigma_{xz} \\ \sigma_{xy} \end{bmatrix}_k = [\bar{Q}]_k \begin{bmatrix} \epsilon_x \\ \epsilon_y \\ \epsilon_z \\ \epsilon_{yz} \\ \epsilon_{xz} \\ \epsilon_{xy} \end{bmatrix}_k$$

Where Q_{ij} are defined earlier.

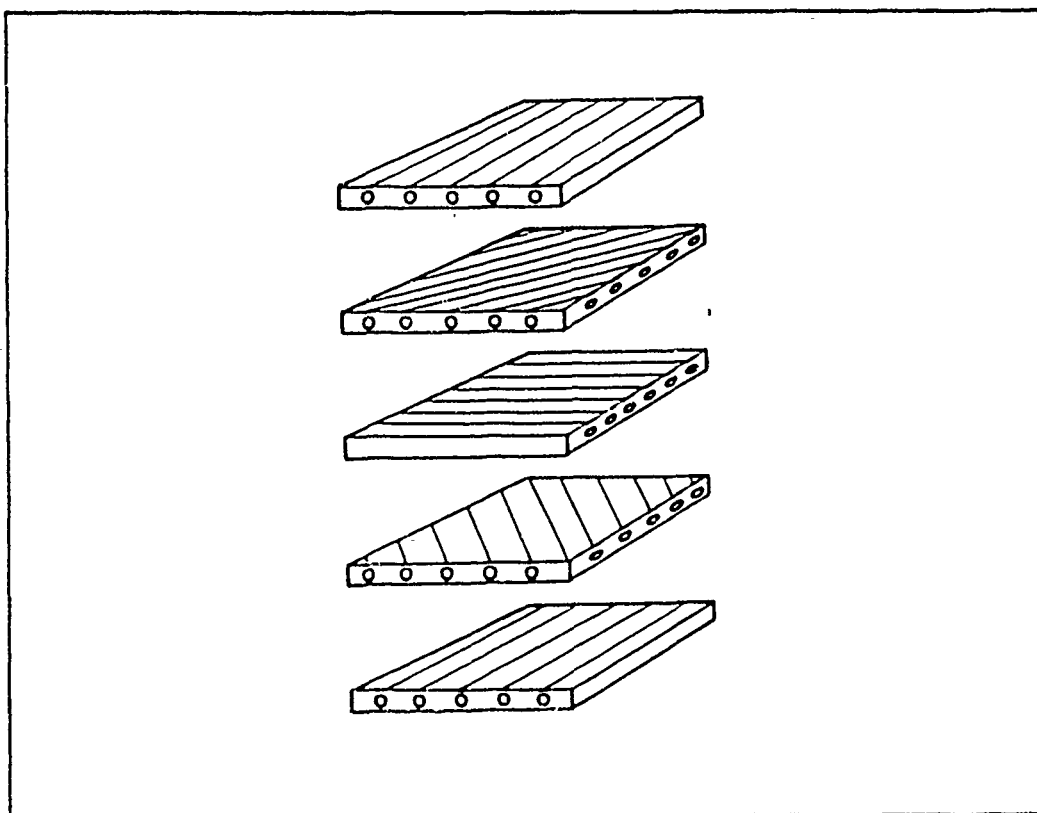


Figure 2 Laminate construction, $[90^\circ/+45^\circ/0^\circ/-45^\circ/90^\circ]$ characterized in this case to show the nomenclature for the lay-up.

C. LAMINATE ANALYSIS

When two or more laminae are bonded together to obtain an integral structural component, the laminae principal material directions are established to produce a component that can resist loads in several directions (Figure 2).

The following procedures enable to obtain the stiffness matrix of such a composite material from the lamina properties, using arbitrary combinations of materials and layer angles.

For the k^{th} lamina of a N layer laminate, equation (11) represents the stress-strain relations.

In order to obtain the strain-displacement relation, the displacements are defined as follows:

$$\begin{aligned} u(x, y, z) &= u_0(x, y) + za(x, y) \\ (12) \quad v(x, y, z) &= v_0(x, y) + z\beta(x, y) \\ w(x, y, z) &= w(x, y) \end{aligned}$$

where u , v and w are displacements in x , y and z directions respectively

and⁴

$$(13) \quad \alpha = - \frac{\delta w}{\delta x} \quad \text{and} \quad \beta = - \frac{\delta w}{\delta y}$$

are the negative of the slope, related to the rotations.

The mid-surface strains, then are given by

$$(14) \quad \epsilon_{x_0} = \frac{\delta u_0}{\delta x}, \quad \epsilon_{y_0} = \frac{\delta v_0}{\delta y},$$

$$\epsilon_{xy_0} = \frac{1}{2} \left[\frac{\delta u_0}{\delta y} + \frac{\delta v_0}{\delta x} \right]$$

while the curvatures are given by

$$(15) \quad K_x = \frac{\delta \alpha}{\delta x}, \quad K_y = \frac{\delta \beta}{\delta y}$$

$$K_{xy_0} = \frac{1}{2} \left[\frac{\delta \alpha}{\delta y} + \frac{\delta \beta}{\delta x} \right]$$

⁴ In the following expressions δ means partial derivative.

Defining h as laminate thickness, h_k (Figure 3) as the vectorial distance from the panel mid-plane, N, M, Q as stress resultants (Figure 4), stress couples and shear resultants respectively. Relations can be established relating these resultants to the strains and curvatures. This matrix is henceforth referred as the ABD matrix.

This nomenclature is adopted for clarity and simplicity as may be noted from the expressions that follow.

The stress resultants are expressed by integrating stresses across the thickness of the plate and is given by:

$$(16) \quad \begin{bmatrix} N_x \\ N_y \\ N_{xy} \\ Q_x \\ Q_y \end{bmatrix} = \int_{-h/2}^{+h/2} \begin{bmatrix} \sigma_x \\ \sigma_y \\ \sigma_{xy} \\ \sigma_{xz} \\ \sigma_{yz} \end{bmatrix} dz$$

and the moment resultants take the following form

$$(17) \quad \begin{bmatrix} M_x \\ M_y \\ M_{xy} \end{bmatrix} = \int_{-h/2}^{+h/2} \begin{bmatrix} \sigma_x \\ \sigma_y \\ \sigma_{xy} \end{bmatrix} z \, dz$$

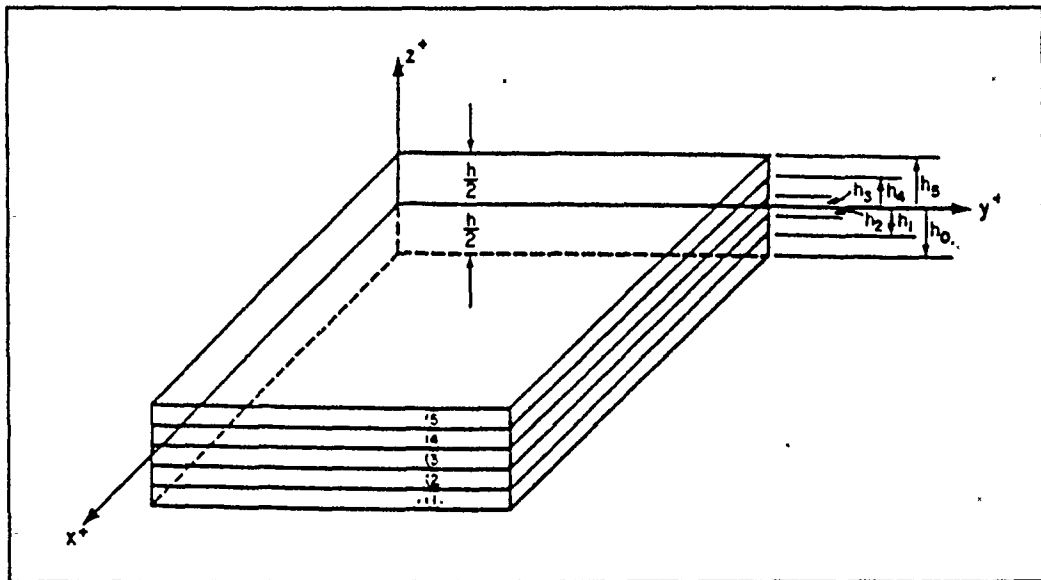


Figure 3 Nomenclature for the Stacking Sequence [Vinson,1987].

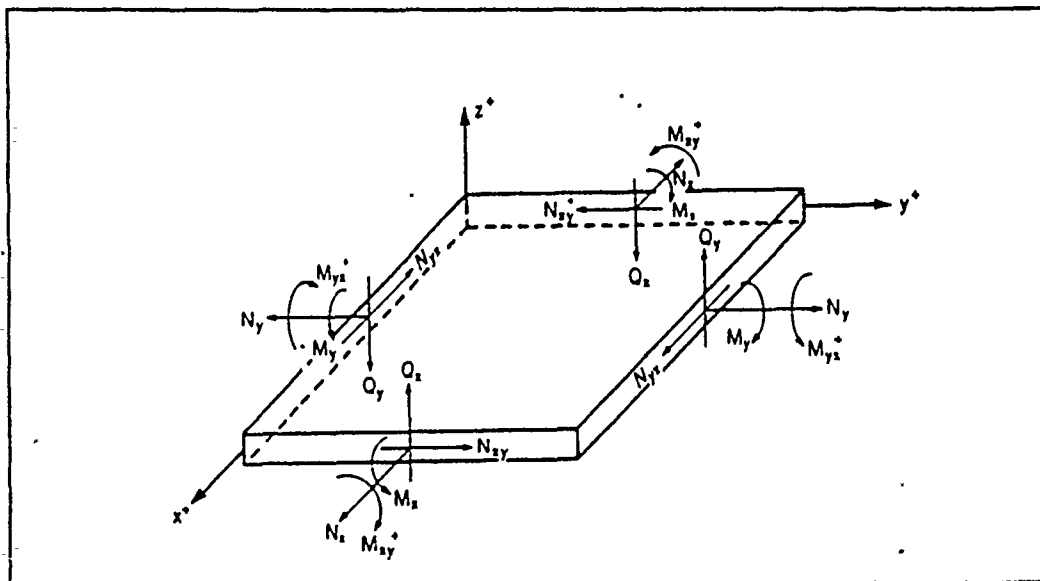


Figure 4 Positive directions for Stress Resultants and Stress Couples for a Plate [Vinson,1987].

Relating resultants with the inplane strains and curvatures through expressions (11) through (14), matrix form is given by:

$$[N] = [A].[ε_0] + [B].[K] \quad (18)$$

$$[M] = [B].[ε_0] + [D].[K]$$

In expression (18), the matrices A, B and D are called extensional stiffness matrix, bending-stretching coupling matrix and flexural stiffness matrix respectively, where:

$$\begin{aligned} A_{ij} &= \sum_{k=1}^N (\bar{Q}_{ij})_k [h_k - h_{k-1}] \quad [i,j=1,2,6] \\ B_{ij} &= \frac{1}{2} * \sum_{k=1}^N (\bar{Q}_{ij})_k [h_k^2 - h_{k-1}^2] \quad [i,j=1,2,6] \\ D_{ij} &= \frac{1}{3} * \sum_{k=1}^N (\bar{Q}_{ij})_k [h_k^3 - h_{k-1}^3] \quad [i,j=1,2,6] \end{aligned} \quad (19)$$

Assuming that transverse shear stresses are distributed parabolically (even though there exists discontinuities at the laminae interfaces), the shear resultants may be written as:

$$\begin{aligned} Q_x &= 2(A_{55}ε_{xz} + A_{45}ε_{yz}) \\ Q_y &= 2(A_{45}ε_{xz} + A_{44}ε_{yz}) \end{aligned} \quad (20)$$

where

$$(21) \quad A_{ij} = \frac{5}{4} \sum_{k=1}^N (\bar{Q}_{ij})_k \left[h_k - h_{k-1} - \frac{4}{3} * (h_k^3 - h_{k-1}^3) * \frac{1}{h^2} \right]$$

$i, j = 4, 5 \text{ only}$

The stresses and moments resultants can be written in a compact form that is very convenient to see the overall relations within a composite material laminate, specifically the ABD matrix. The ABD matrix is obtained as a combination of the expressions in (18). Expressions (18) and (22) are equivalent and in expression (22) the ABD matrix is defined explicitly.

$$(22) \quad \begin{bmatrix} N_x \\ N_y \\ N_{xy} \\ M_x \\ M_y \\ M_{xy} \end{bmatrix} = \begin{bmatrix} A_{11} & A_{12} & A_{16} & \vdots & B_{11} & B_{12} & B_{16} \\ A_{12} & A_{22} & A_{26} & \vdots & B_{12} & B_{22} & B_{26} \\ A_{16} & A_{26} & A_{66} & \vdots & B_{16} & B_{26} & B_{66} \\ \bar{B}_{11} & \bar{B}_{12} & \bar{B}_{16} & \vdots & \bar{D}_{11} & \bar{D}_{12} & \bar{D}_{16} \\ B_{12} & B_{22} & B_{26} & \vdots & D_{12} & D_{22} & D_{26} \\ B_{16} & B_{26} & B_{66} & \vdots & D_{16} & D_{26} & D_{66} \end{bmatrix} * \begin{bmatrix} \epsilon_{x_0} \\ \epsilon_{y_0} \\ \epsilon_{xy_0} \\ K_x \\ K_y \\ K_{xy} \end{bmatrix}$$

D. EFFECTS OF PLY ANGLE θ

To get an insight of the overall influence of the ply angle θ on the laminate stiffness, it is useful to observe the effects of θ for a given lamina. As each element of the ABD matrix, A_{ij} , B_{ij} , and D_{ij} , is a function of the material stiffness coefficient \bar{Q}_{ij} , the layer thickness t_k and mid-plane

vectorial distance h_k , the \bar{Q}_{ij} 's represent the stiffness variations due to ply angle changes in a given lamina.

The property of the composite material that reveals its advantages over metallic or plastic is that it can be tailored to fit a given structural shape and a specific set of loads and operating conditions.

The terms of the ABD matrix are functions of the material properties and the ply angle θ . If the properties are kept constant and within typical values of most fiber resin types of composite, it is possible to plot the values of \bar{Q}_{ij} versus θ and get a set of seven very useful graphs. These will permit an initial appreciation of such effects, and how they can be combined to meet a specific structural requirement.

Figures 5 to 11 show how the elements of the "material stiffness" matrix ABD can be tailored by changing the ply angle, taking full advantage of this characteristic behavior of laminated composite material.

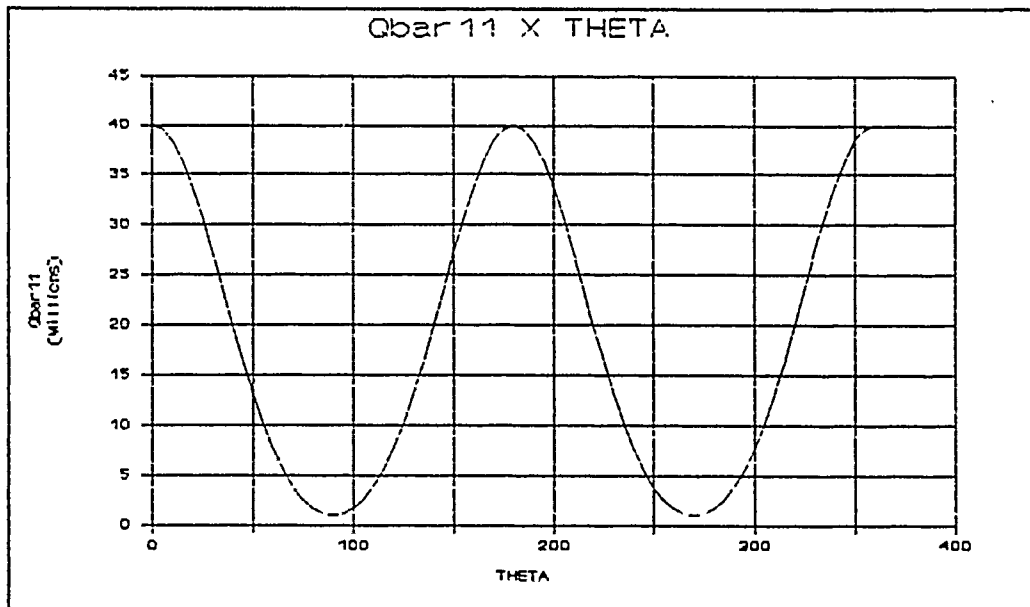


Figure 5

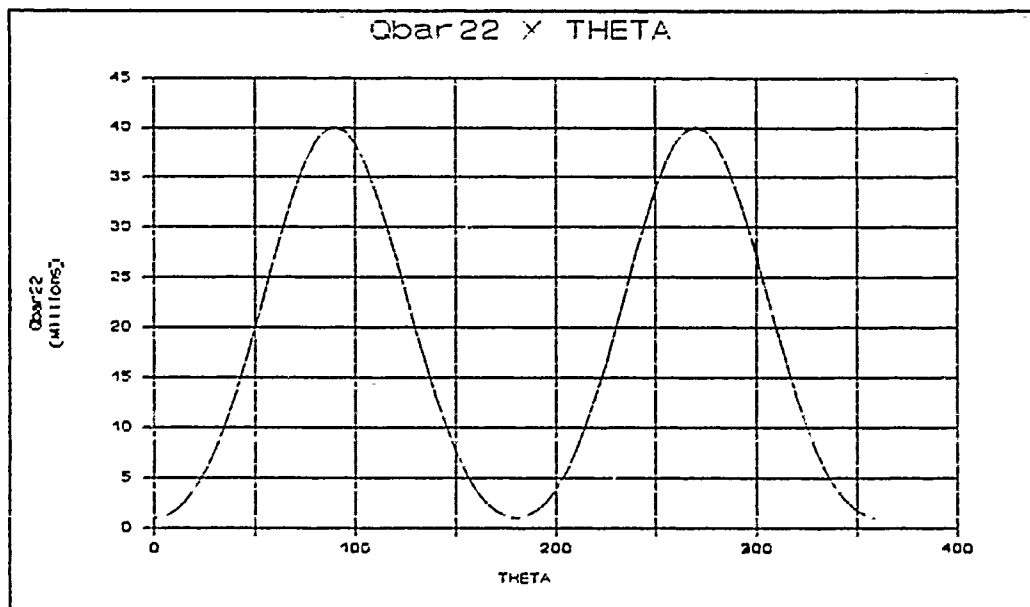


Figure 6

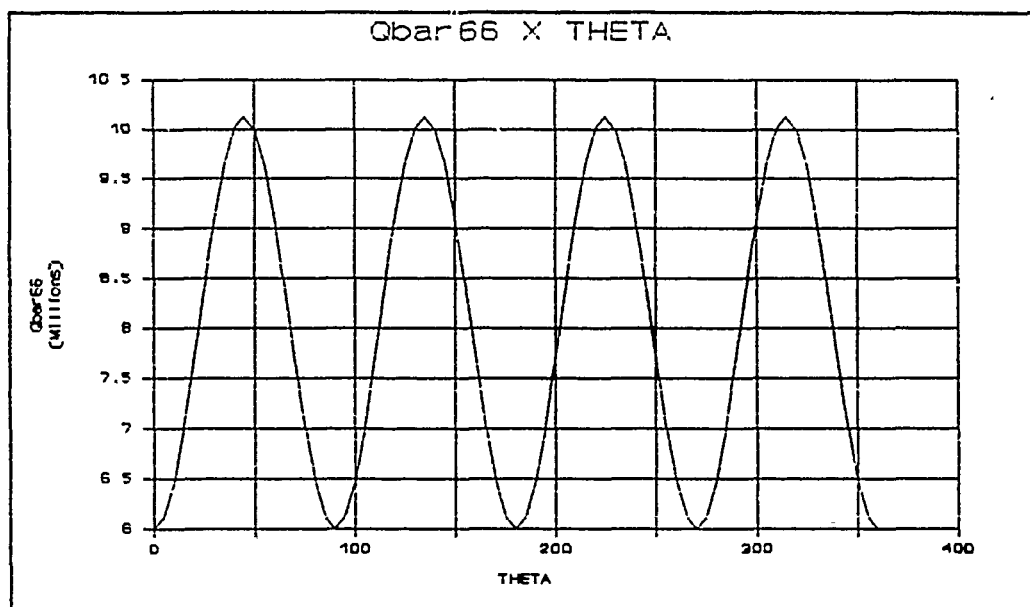


Figure 7

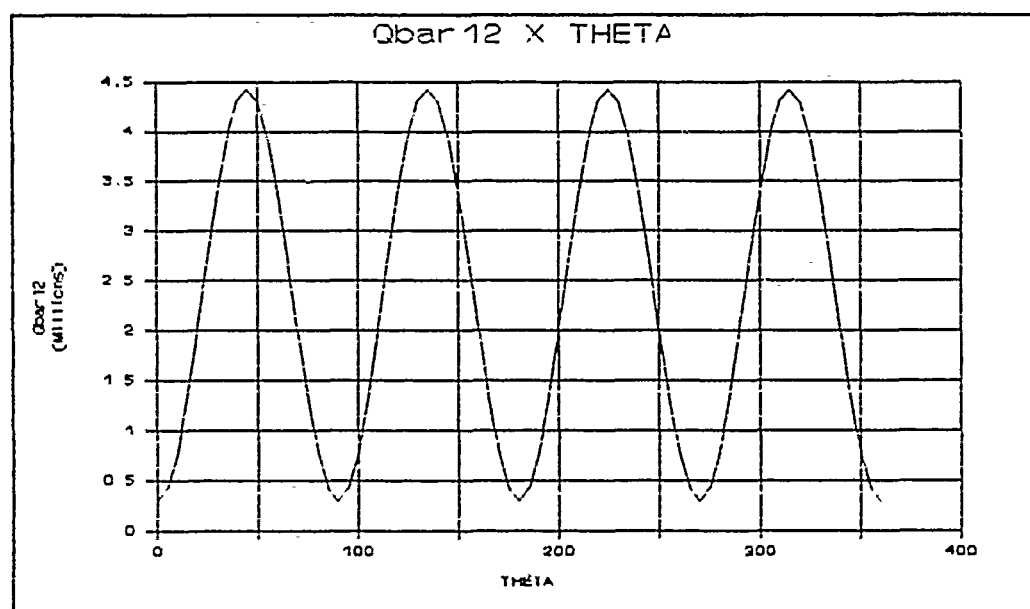


Figure 8

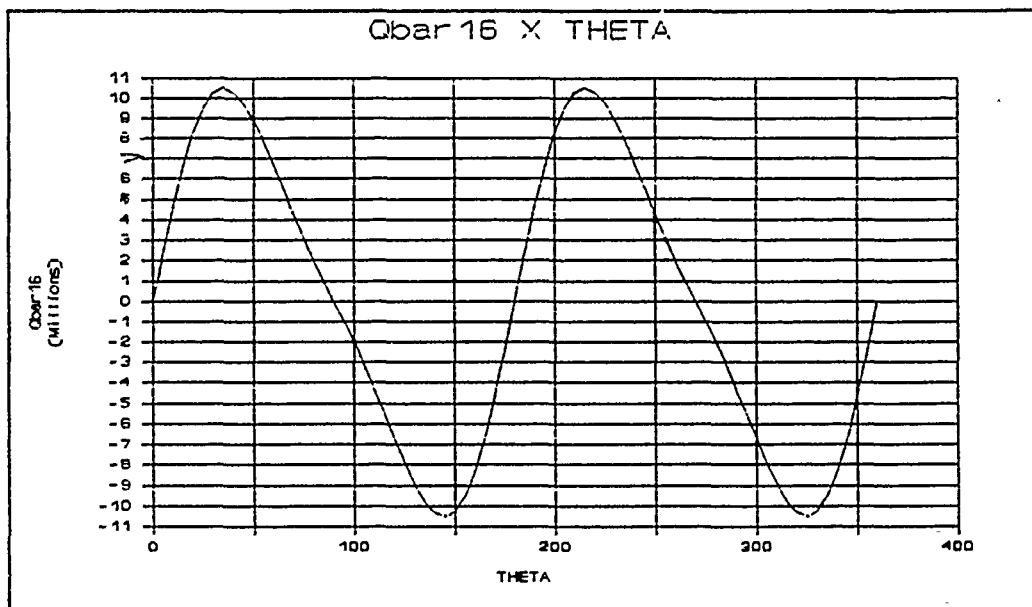


Figure 9

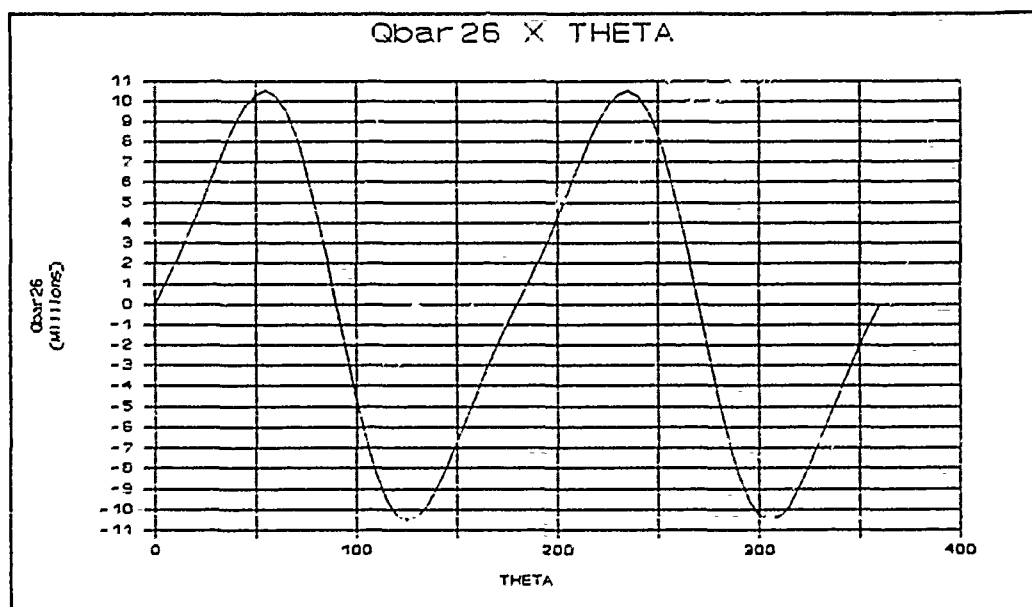


Figure 10

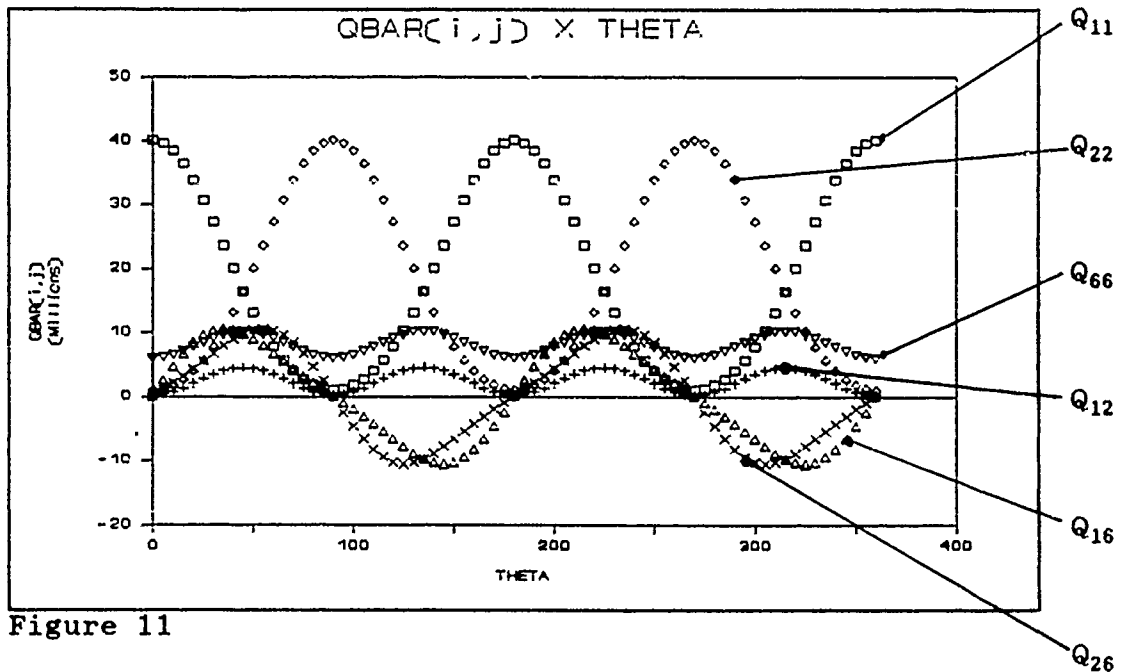


Figure 11

In figure 11 all Q 's are superimposed, on the same plot, to give a better perspective of the trends in doing this kind of layer design to fit specific structural constraints. When A_{16} and A_{26} are non-zero there is stretching-shearing coupling, while non-zero B_{16} means twisting-stretching coupling, and non-zero B_{26} indicates bending-shearing coupling; bending-twisting coupling is originated in non-zero values of D_{16} and D_{26} .

In normal design procedures, these terms are made zeroes by selecting appropriate stacking sequence; cross ply ($0^\circ/90^\circ$ plies combination) or angle ply laminates ($-\theta/+\theta$ plies combination). Other important factor to be considered is the symmetry with respect to the mid-surface plane.

The stress strain relations or constitutive relations (ABD matrix), combined with the proper equations of equilibrium and the strain-displacement relations form the basis for analyzing beams, plates or shells.

These basic relations lead to the motivation and reasoning behind the model tailoring to fit a design requirement.

III. ROTOR MODELING

A. TYPICAL CURRENT ROTOR MODELING

Current rotor design is a compromise between the different requirements in hover and forward flight, and the analytical models reflect that tendency or limitation. For instance, the optimum twist for hover is not the same in forward flight for tilt rotors as well as for helicopters. Indeed, very often, the designers avoid extension-twist coupling with laminated composite materials because of certain undesirable effects. The result is that one of the two flight modes will have less than optimal propulsive efficiency, depending on design phase decisions driven by requirements and/or aircraft mission profiles.

With the tilt rotor concept of mixing fixed wing and rotorcraft technology, these design trends were brought to surface once more.

B. PROPOSED SOLUTION

Nixon[1987] proposed a solution for this sort of dilemma. The model used an extension-twist coupled rotor blade with

100% RPM⁵ in hover and 80% RPM in forward flight. These are reasonable ratios between hover and forward flight for a tilt rotor type aircraft. The difference in RPM provides a change in centrifugal force, inducing a change in the twist angle distribution, which can be used to optimize the rotor for both regimes.

The use of composite materials makes it possible to design a rotor blade that takes advantage of the changing loads, rendering the required twist distribution optimum in each flight mode. At this point one question arises:

What is the magnitude of twist available from a particular geometry and material system?

The answer to that question lies in a method of prediction, with a model that behaves as close to the actual blade as possible yet inexpensive enough to permit a wide spectrum parametric study, providing a source to evaluate several geometry and material systems. Certainly such modeling should be verified by experimental data.

This research is aimed to address the analytical part of the above question and provide design tools to rotor blade systems.

⁵ Reference value for 100% RPM is 217 rad/s, in that scale of rotor blade.

The torsional moments that affect a rotating blade can modify substantially the twist distribution.

In this numeric model, the pitching moments generated by aerodynamic loading are not taken into account, the emphasis being on the inertia and extension-twist coupling as sources of torsional moments.

An assumed lift distribution acts on the model, but compared with the inertia forces, its effects are negligible on the rotating blade. The inertia forces acting on the rotating blade produce extension which causes twist by structural coupling. However, the same inertia forces produce a centrifugal flattening [Prouty, 1986] effect called *tennis racket effect* (because of the tendency of a tennis racket to align its plane with the plane of rotation as it is swung in an arc).

The forces acting in a helicopter blade can be seen in Figure 12, and it may be noted that in this case the effect is reduced with balancing weights (Chinese weights).

C. GIFTS CAPABILITIES

Gifts capabilities include generation of any type of structural model, with the following elements:

- . one-dimension rods or beams
- . two-dimension plates

. three-dimension shells, solid and complex stiffened shells.

The elements can be selected from a library of options.

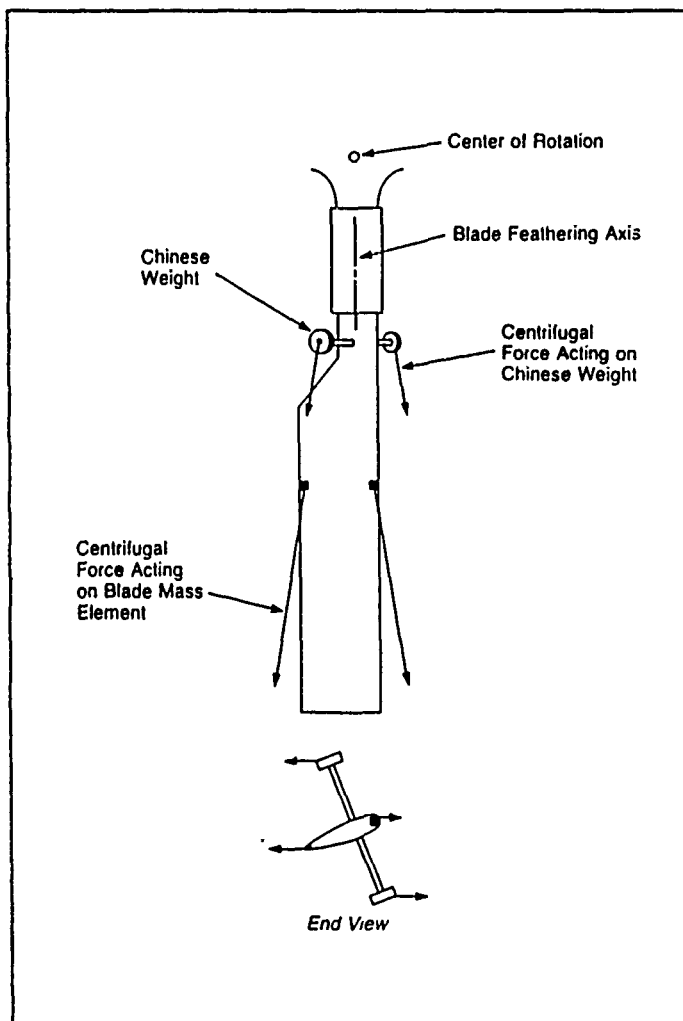
The materials can be created by the user or selected from a library of standard definitions. The program allows the user to define isotropic materials and laminated composite materials, that can have up to a maximum of hundred layers.

Loads can be concentrated or distributed, static as well as function of time.

Static and dynamic analysis are performed on the models generated. The dynamic analysis provides free vibration response and forced response (transient computations), and model superposition.

In using GIFTS as the finite element program to model the blade, the effects of the centrifugal force are taken into account with the forces acting on the lumped masses as shown in Figure 12, radially from the center of rotation. In using other finite element programs this feature must be verified for correct usage and application. The tennis racket effect can affect the twist angle to a large extent. If the centrifugal forces act in parallel lines instead of passing through the center of rotation, there will be no centrifugal flattening effect and results in larger twist angles.

The basic rotor model selected to apply the proposed method is the one analyzed by Hodges[1987], this model was analyzed using two different methods, namely by finite element



(MSC/NASTRAN) and a coupled-beam model [Rehfield, 1985]. The rotor geometry presented by Hodges[1987] was modeled in GIFTS using triangular TB3 element ("flat triangular plate or shell element, including membrane, out of plane and fictitious in-plane bending stiffness." [Batoz, 1980])). The results indicated a wide

Figure 12 *Twisting Moments Due to disparity of results. Centrifugal Forces [Prouty,1986].* However, the present model appears to be within the assumption of linear and small displacements theory.

The models in Figure 13 have a notation (M_{120} / M_{1-20}) that is described in the next section. A twist angle distribution discrepancy could be explained by the tennis racket effect probably not present in the model described in

Hodges[1987], but the tip vertical displacement due to lift and weight with no rotation could not be explained by this argument. It may be observed that the displacements quoted in the referenced work are about 25% of the length, which appears to violate the linear theory that was used.

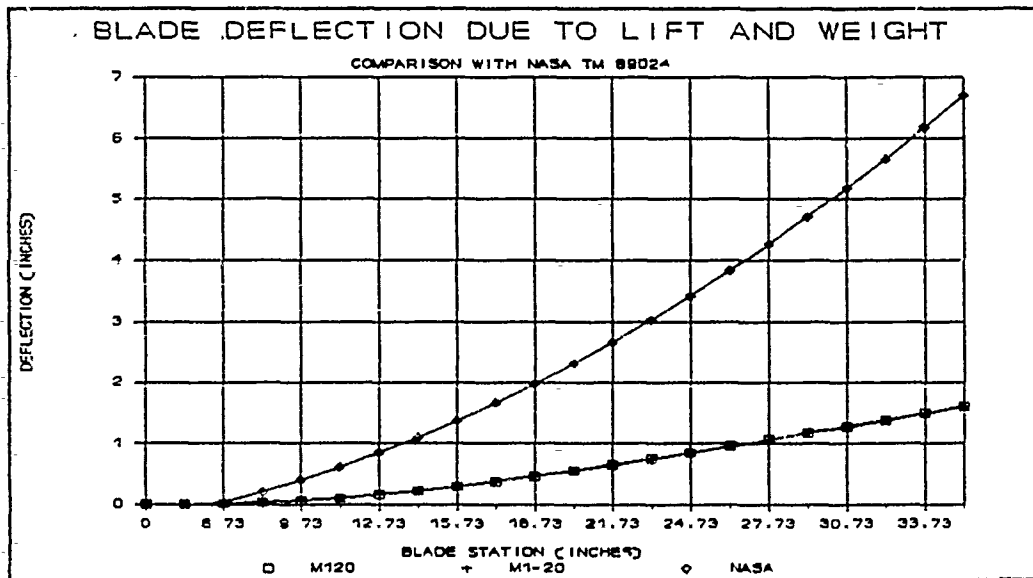


Figure 13 Comparison between GIFTS model and NASA TM 89024 results.

This discrepancy may be due to a possibility that the models compared are not exactly the same, although every effort was made to take into account all the pertinent

geometric and material data reported. However this discrepancy was the driving factor that raised some questions, such as:

What are the possibilities to model different structural configurations starting with the same number of layers, same lay-up design, same thickness and material properties? (perhaps by inadvertent oversight by the designer, analyst using canned programs, or manufacturing engineer.)

The answer to this was based on the following assumptions:

- . The structure is a D shape spar.
- . It is built using three shells, top, bottom and rear shell surfaces .
- . The top and bottom meet at the leading edge and the rear shell closes the box.
- . Once established, the internal lay-up in the stacking sequence remains constant.

With those assumptions a laminate to constitute one shell surface may be defined, using only the Laminate Principal Orientation (LPO) angle. For example, in the following laminate $[+20^\circ/-70^\circ/+20^\circ/-70^\circ/-70^\circ/+20^\circ]$, the top layer angle is denoted $+20^\circ$ and is a six layer asymmetric laminate.

Rotating the whole laminate 40° clockwise gives $[-20^\circ/+70^\circ/-20^\circ/+70^\circ/+70^\circ/-20^\circ]$, whose Laminate Principal Orientation angle is denoted as -20° .

This laminate has intentionally designed asymmetry to get the extension-twist coupling. Associated with this laminate

is a normal vector whose orientation is seen in Figure 14. The D-spar then is built using three such laminates, with each laminate mounted with the normal vector facing inward or outward. This method of construction results in six different configurations of the rotor. These configurations and other variations within each one will be developed in the next section.

D. VARIOUS ROTOR DESIGNS OR CONFIGURATIONS

The six different configurations are designated M1 to M6 and the LPO⁶, varying from -90° to $+90^\circ$ in steps of 20° , provides the suffix to complete the model designation M1-90⁷, M340, M6-60 etc. In a total of 11 LPO in each model.

Different configurations may be visualized with the help of the scheme shown in Figure 14.

Model I and IV can be built with only one laminate wrapped around, one inverse of the other.

In the program GIFTS, the outward vector for each surface is defined during the "GRID" definition, e.g. in a four sided grid, each shell is defined within a grid. The local X axis

⁶ Laminate Principal Orientation Angle, referred to the top layer of the laminate used to construct that particular model.

⁷ M1-90 meaning model 1 with LPO = -90° ; M340 meaning model 3 with LPO = 40° .

is oriented parallel to the first line of the grid, the local Z axis is the cross product of the first and second "line" in the grid definition, while the local Y axis is the cross product of the Z and X axes, as is usual in cartesian systems.

The outward vector is oriented in a direction defined by the local Z axis. Layer angles are positive in the counter-clockwise direction in the XY plane for shell elements, as is the convention for laminated composite materials.

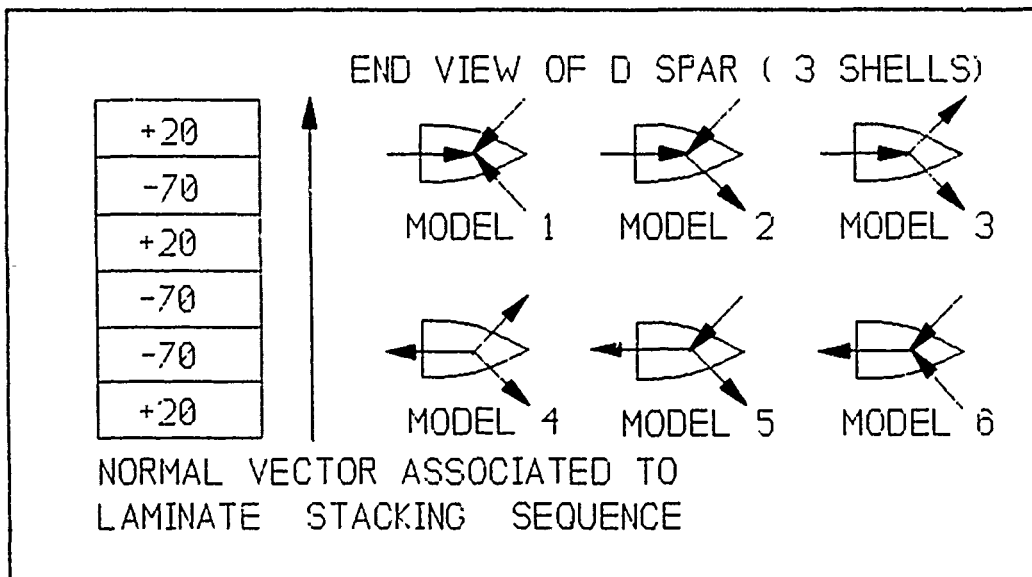


Figure 14 Normal to surface vector associated with the layer sequence of the basic laminate and its position in relation to end view of the blade.

It may be observed that, when an asymmetry is present in the basic laminate (material definition), the structural

response is highly dependent on how the grid and consequently the lay-up is defined. In the case of a symmetric laminate or isotropic material, this fact is never brought to surface because of its irrelevancy. However, dealing with asymmetric laminated composite materials, the analyst must always have this in mind. It may be noted that, in most cases the laminate is chosen to be symmetric.

Table 1 gives in a compact form the description of various laminate constructions described. Included in that table are the line names actually employed in the input file M\$**.SRC [Annex 1] (\$ = 1,2,3,4,5,6 models; ** = top layer angle as defined previously, in the range -90 to +90), to develop the models generated in GIFTS. By modifying two areas in this input file, six models are generated that are considered under the present study, this also provides variation of the layer angle within each model. The actual modifications employed in the input file are given in LAYUP.AUX [Annex 2]. For each model (one of the six combinations obtainable by the change in the laminate associated vector, as given in Figure 14), the whole laminate was rotated in increments of 10°, referenced to the top layer angle (LPO). For each of these models, the RPM, and consequently the centrifugal force, was varied in the range (130 rad/s to 300 rad/s).

The model geometric characteristics are the same as in Hodges[1987], a graphite epoxy composite rotor blade constructed out of Hercules IM6 fiber with Ciba-Geigy R6376

resin. The cured ply thickness is assumed to be 0.0055 in. The D-spar has a 35.23 in. radius, and begins at station 5.32 in., which has all degrees of freedom suppressed to emulate a rigid rotor connection to the hub. The rotor has a constant cross-section, defined by 13 nodes and is divided into 21 span-wise (3.0 in apart) stations. Models with finer meshes were used in the early stages to check for convergence. The mesh selected seemed to be a reasonable compromise between the computational time and accuracy.

The orthotropic material properties of the lamina are listed below:

E_{11} ,psi.....	23.1×10^6
E_{22} ,psi.....	1.4×10^6
ν_{12}	0.338
G_{12} ,psi.....	0.73×10^6

TABLE 1 - MODEL DEFINITION:

Example		GRIDS, POINTS AND LINES							
Vector		5	L45	4	L14	1	L51	5	
+20	↑	L512	G3	L411	G1	L18	G2	L512	
-70									
+20									
-70									
-70									
+20									
		12	L1112	11	L811	8	L128	12	
(not to scale, e.g. line L512 is 30.0 in length, L45 is .286 in, and L14 is about 1.15 in)									
* = vector inward ; o = vector outward.									
POSSIBLE		RIGHT HAND RULE NORMAL VECTOR TO SURFACE							
MODELS		GRID DEFINITION							

M1\$\$	VECTOR	*	*	*
	GRID DEF.	L512,L1112,L411,L45//	L411,L811,L18,L14//	L18,L128,L512,L51//
M2\$\$	VECTOR	*	*	o
	GRID DEF.	L512,L1112,L411,L45//	L411,L811,L18,L14//	L512,L128,L18,L51//
M3\$\$	VECTOR	*	o	o
	GRID DEF.	L512,L1112,L411,L45//	L18,L811,L411,L14//	L512,L128,L18,L51//
M4\$\$	VECTOR	o	o	o
	GRID DEF.	L411,L1112,L512,L45//	L18,L811,L411,L14//	L512,L128,L18,L51//
M5\$\$	VECTOR	o	o	*
	GRID DEF.	L411,L1112,L512,L45//	L18,L811,L411,L14//	L18,L128,L512,L51//
M6\$\$	VECTOR	o	*	*
	GRID DEF.	L411,L1112,L512,L45//	L411,L811,L18,L14//	L18,L128,L512,L51//

IV. STATIC AND DYNAMIC ANALYSIS

The six models described in chapter III are basically subjected to three main types of independent static loads. Further, a modal analysis is also performed to obtain the first four fundamental modes of vibration frequencies and mode shapes.

The first load applied is a torque at the tip, not combined with any other load.

The second load case consists of combined lift and blade weight at zero RPM, i.e. with no centrifugal forces.

The third load case is the centrifugal force due to rotation of the blade. The lift and blade weight are present and the RPM varies from 130 rad/s to 300 rad/s.

A. TORSIONAL LOAD

A moment of 26.4 in-lb is applied distributed among the nodes at the tip as concentrated moments.

This load case reveals the influence of the laminate principal orientation angle (LPO), and the torsional stiffness for each model. The different response of the six different models also is presented for comparison purposes.

The results are presented in Figure 15 for the six models for LPO's of +20° and -20° in each model.

As much as 40% variation in the response may be observed in the comparisons.

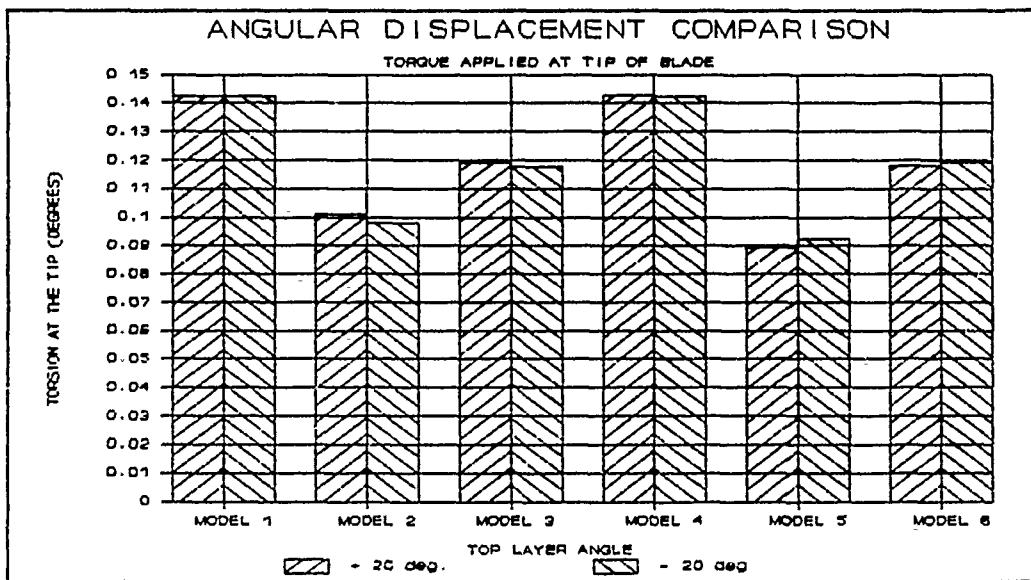


Figure 15 Angular Displacement at the Tip Due to Pure Torque.

B. LIFT AND BLADE WEIGHT LOADS

This loading is designed to get the combined effect of the lift and blade weight given by Hodges[1987], expressed in terms of radial distance of the center as follows:

$$(17) \quad l = (0.02222 \text{ lb/in}) \times r - 0.0123 \text{ lb/in}$$

This load is applied vertically in two spanwise rows at the leading and trailing edges, in a proportion that produces zero moments at the quarter chord. This load distribution is more homogeneous and induces less cross-section distortion, as opposed to the application along a line on upper surface as in beam type elements. This distributed line loading produces small torsional displacement (10^{-4} degree).

The results are presented in Figure 16 for the six models, with 2 values of LPO (+20° and -20°) for each model.

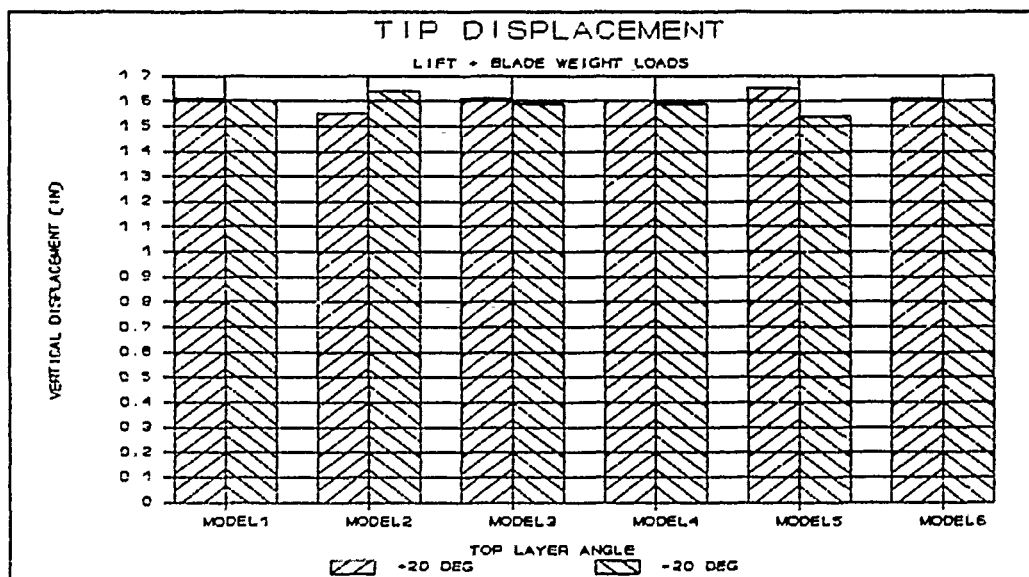


Figure 16 Displacement at the Tip Due to Vertical Loads Along the Blade.

C. CENTRIFUGAL LOAD

Next loading case investigated reveals the effect of varying centrifugal load, combined with changing the LPO angle within each model. The response yields twist angle induced by extension-twist coupling present in the structure due to asymmetric stacking sequence.

The LPO, referred to the top layer angle, varies in the range of $\pm 90^\circ$, the internal lay-up in the stacking sequence remaining constant, as previously defined.

After some experiments to localize inflection points in the twist angle variation, the LPO to be investigated were chosen in the range of $\pm 90^\circ$, giving a total of 11 laminate principal orientation angle for each of the six models.

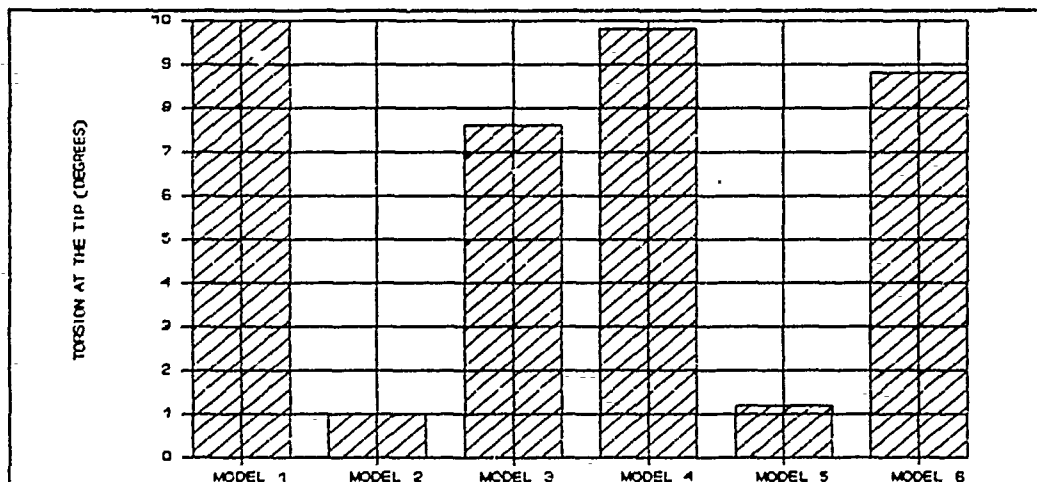


Figure 17 Overall Range of the Twist Angle within the Six Models.

The loads due to lift and blade weight are present but their effects are observed to be negligible compared with those due to centrifugal loads.

The RPM is varied from 130 rad/s to 300 rad/s in increments of 10 rad/s, in a total of 19 load cases. The combination of load cases and LPO give a total of 201 points of twist angle for each of the six models. These points are presented in six 3-D graphs to better appreciate the choices offered in this design approach. Those graphs present the trends of the twist angle with RPM and LPO variations. The twist angle range for each model is in Figure 17, while the overall parametric information are presented in Figures 18 through 23.

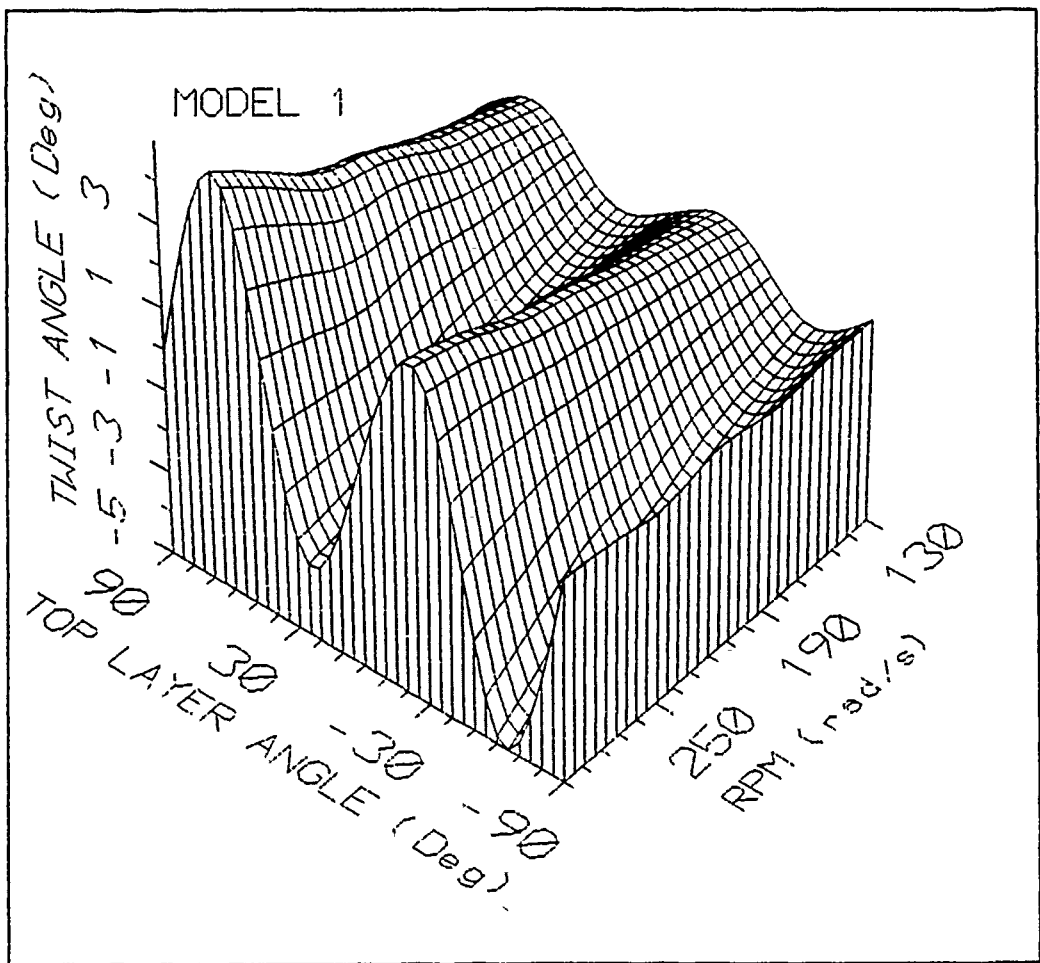


Figure 18 Model One, Twist Angle Induced by Rotational Inertia Loads Combined With Laminate Principal Orientation (LPO), Referred to Top Layer Angle.

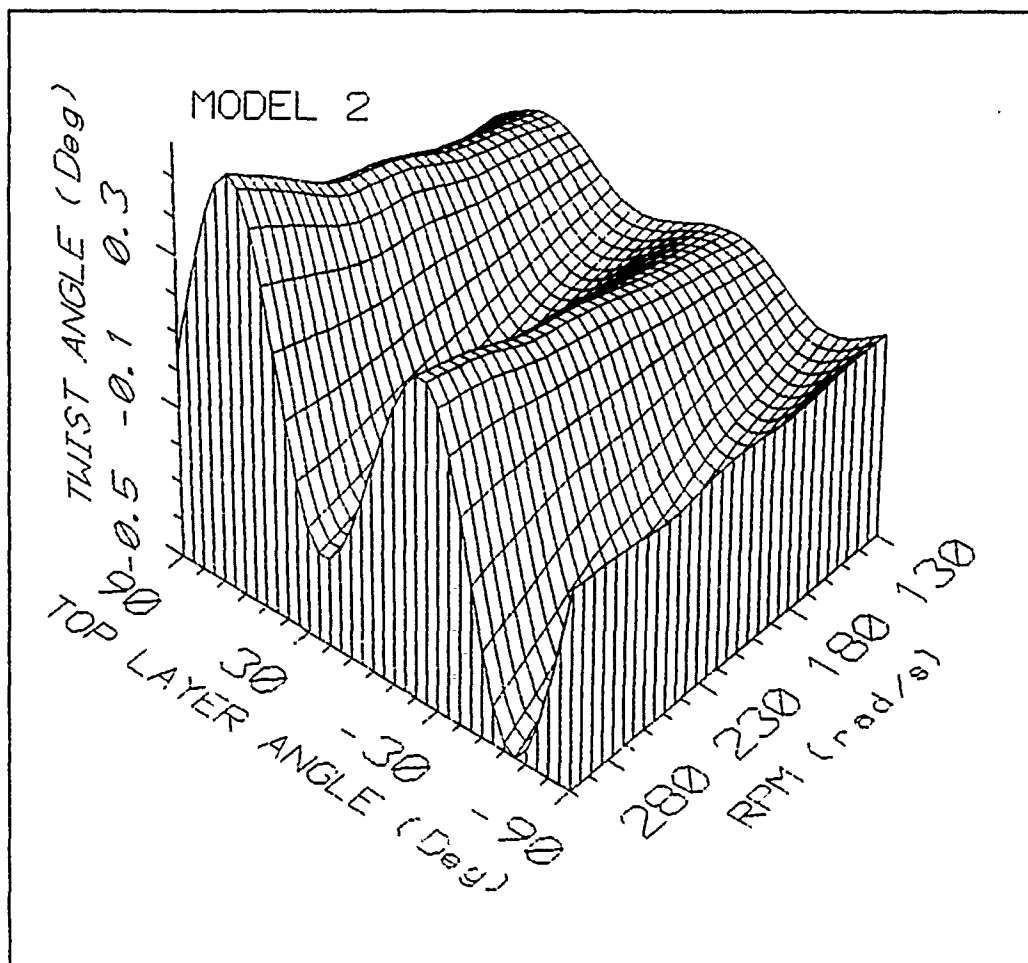


Figure 19 Model Two, Twist Angle Induced by Rotational Inertia Loads Combined With Laminate Principal Orientation (LPO), Referred to Top Layer Angle.

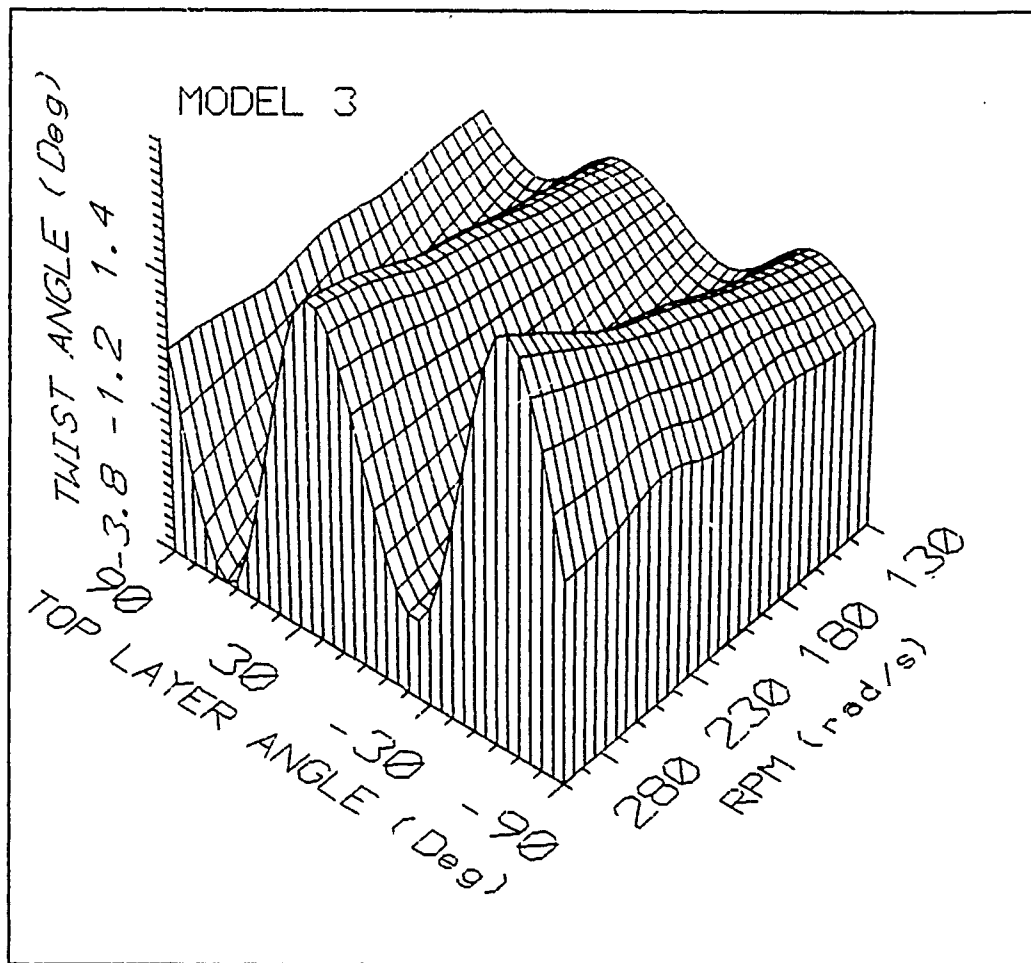


Figure 20 Model Three, Twist Angle Induced by Rotational Inertia Loads Combined With Laminate Principal Orientation (LPO), Referred to Top Layer Angle.

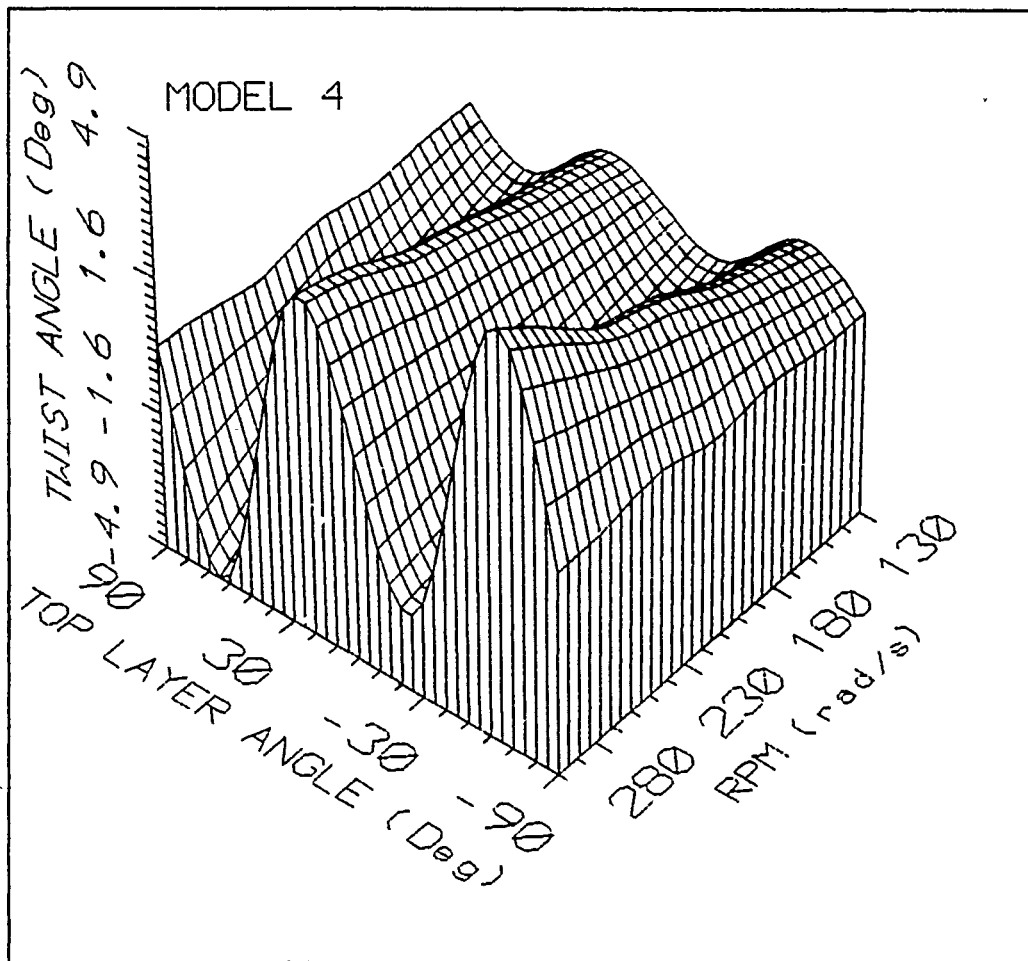


Figure 21 Model Four, Twist Angle Induced by Rotational Inertia Loads Combined With Laminate Principal Orientation (LPO), Referred to Top Layer Angle.

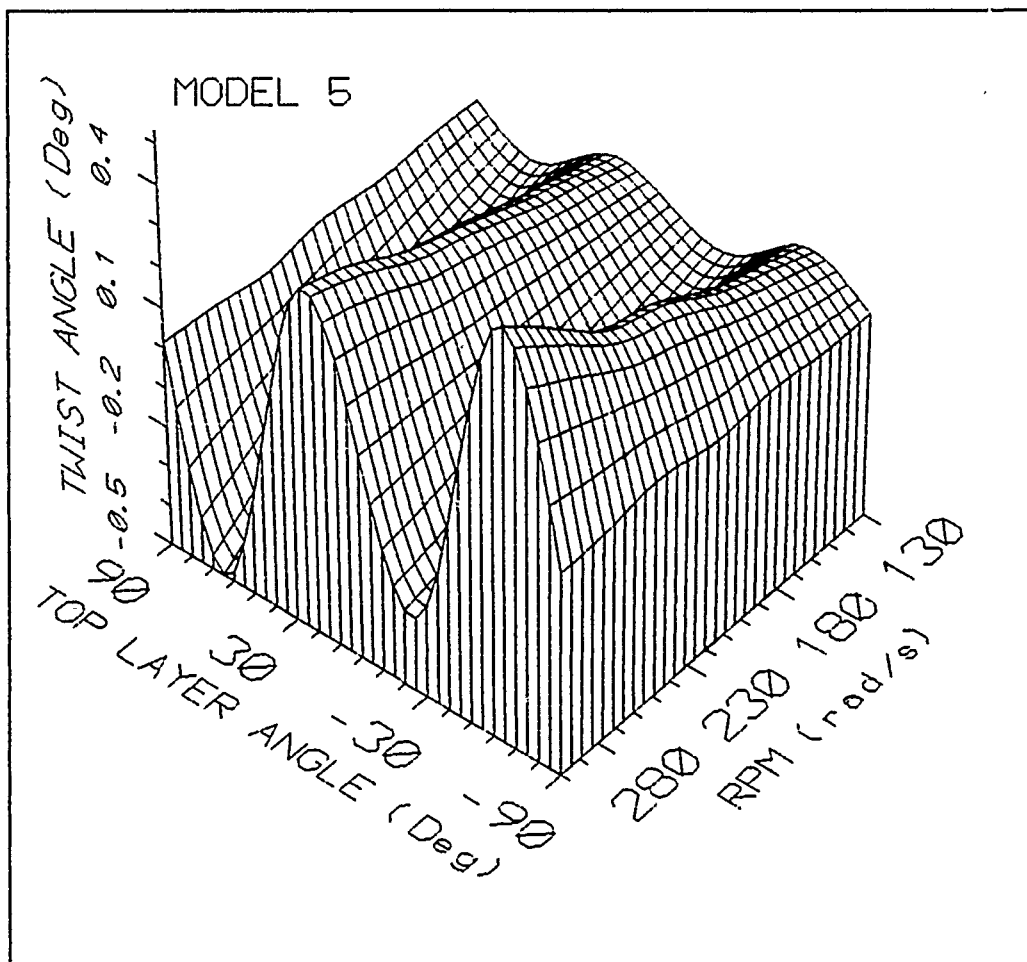


Figure 22 Model Five, Twist Angle Induced by Rotational Inertia Loads Combined With Laminate Principal Orientation (LPO), Referred to Top Layer Angle.

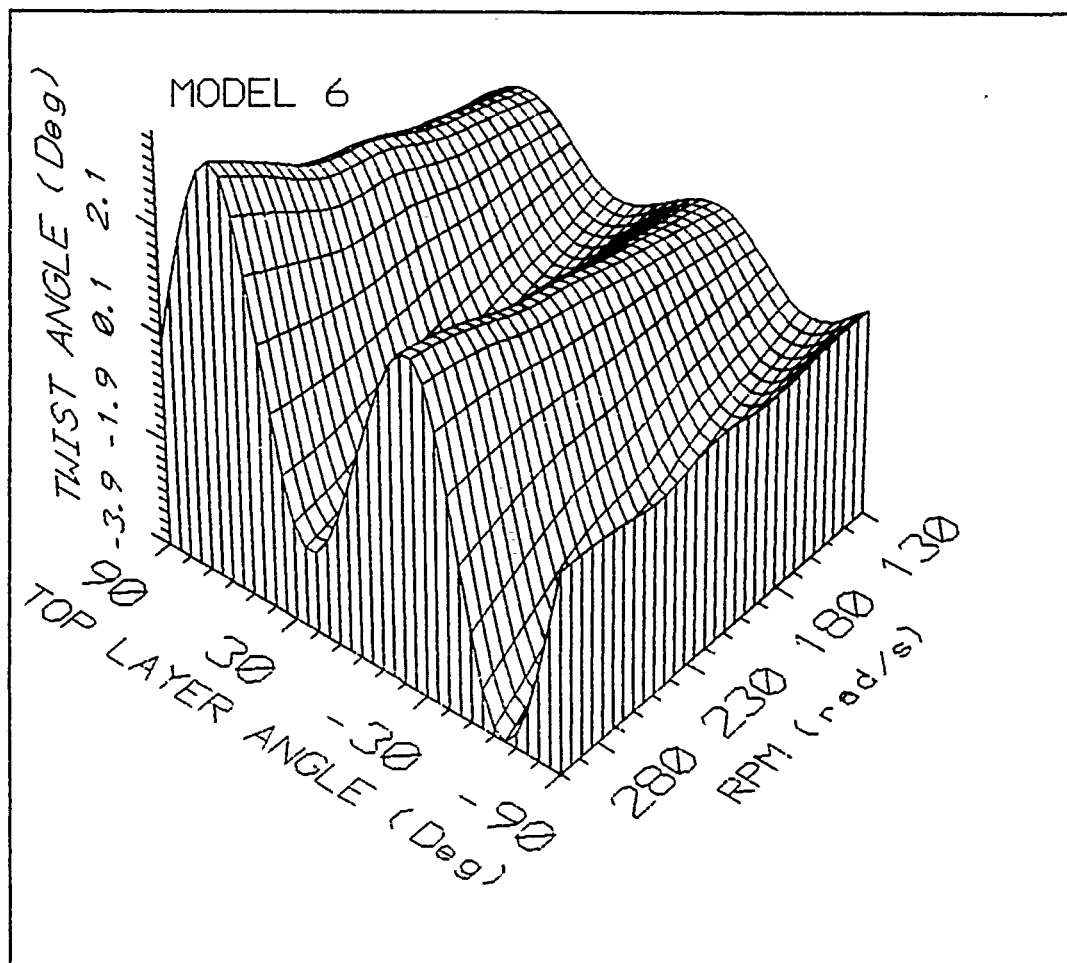


Figure 23 Model Six, Twist Angle Induced by Rotational Inertia Loads Combined With Laminate Principal Orientation (LPO), Referred to Top Layer Angle.

D. MODAL ANALYSIS

To observe the effects of each configuration (Model) and laminate principal orientation on the first four fundamental frequencies, a free vibration analysis is performed.

The results of the modal⁶ analysis are depicted in Figures 24 and 25 for the six models and for LPO's of -20° and $+20^\circ$ respectively.

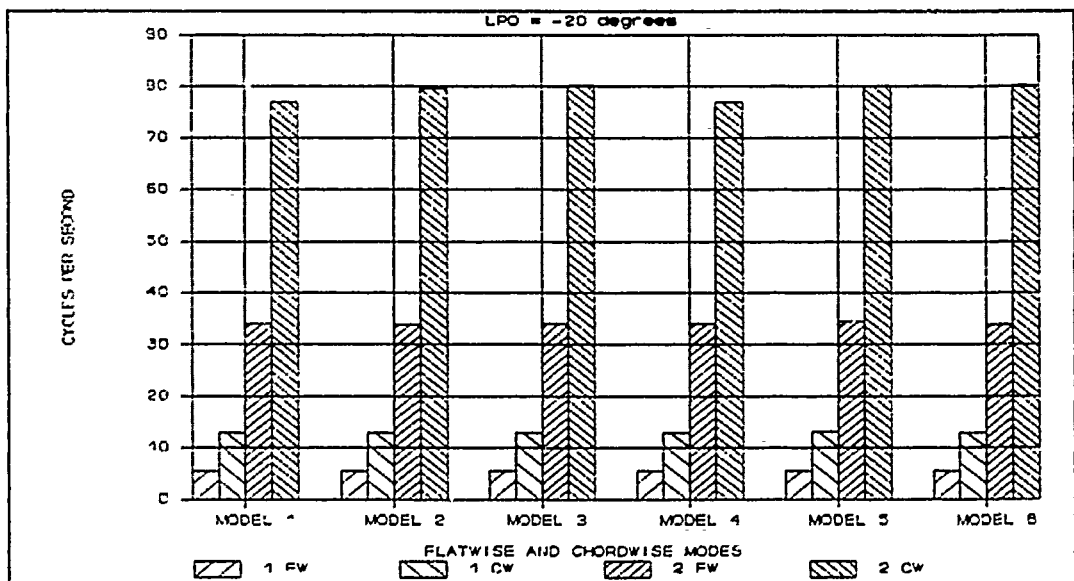


Figure 24 Frequency Variation among Different Models.

⁶ 1 FW means First Flapwise; 1 CW means First Chordwise and so on.

It may be noted that, even for simple models, this solution procedure is a time consuming task, only recommended for final or quasi final configurations in the design process, or using a very crude mesh lay-out.

It can be seen that, for each vibration mode, the frequency remains practically constant. This reveals a low sensitivity of the frequency to changes in model configurations, considering the first four fundamental modes and same LPO's.

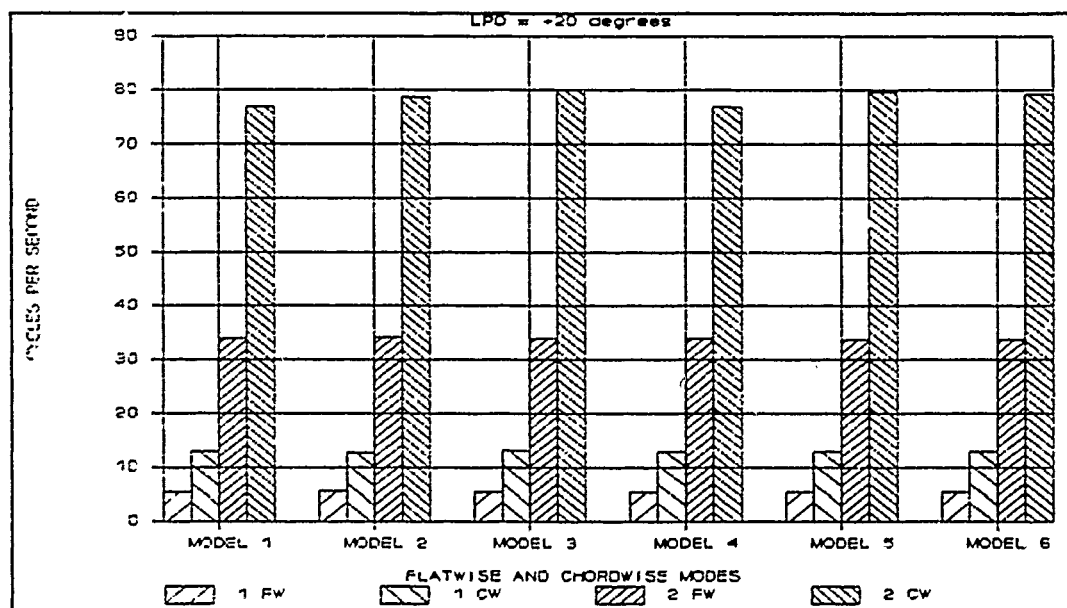


Figure 25 Frequency Variation among Different Models.

V. ANALYSIS OF RESULTS

In this chapter the results obtained for each model will be presented and several observations are inferred.

The present research was conducted to get an insight of the trends implicated into the two questions posed in Chapter III, sections B and C. This study also provides some insight into answering the questions posed in sections B and C of Chapter III.

What is the magnitude of twist available from a particular geometry and material system?

What are the possibilities to model different structural configurations starting with the same number of layers, same lay-up design, same thickness and material properties?

The first question is a design approach to structural analysis. That approach will be elaborated in this chapter.

The second question opened a vast field for research activity that will be addressed in next Chapter.

It can be seen in Figure 14 that the models 1 through 6 are obtained simply by changing one of the normal vectors associated with the laminate, (in one of the three faces of the spar). The effects of these changes in the structural behavior of the blade may be divided into two main categories, static and dynamic behavior.

A. DYNAMIC BEHAVIOR

The free vibration characteristics are shown in Figures 24 and 25. Figure 24 shows the frequencies for LPO of -20° and Figure 25 presents for LPO of 20° . The first four fundamental modes of vibration have very little sensitivity to the model type, and may be observed that the frequencies do not change, for the same or symmetric LPO (positive/negative).

This behavior can be considered benign, or in other words auspicious, in a connotation that, once the designer arrived at the desired frequency values for the RPM range considered, the LPO or the model can be changed until a desired twist-extension coupling is achieved.

These iterations can be done without looking very close to resonance problems, which must be checked anyway when the final model is to be selected.

This assumption is made based on the validity of Yntema[1955] approach for these models. It is possible that the change in the stiffness matrix due to RPM affects the rotor built of laminated composite materials in a different way than isotropic rotors. Further research needs to be done along this direction to obtain comparable results for composite rotors.

In Figures 24 or 25, each column corresponds to one mode of vibration at zero RPM and is a point in the 3-D plot for that specific mode (flatwise, chordwise or pitchwise⁹). The RPM and LPO may be varied as in the static case yielding carpet plots. The resulting plots would validate or not the assumption of Yntema's values for composite blades.

B. STATIC BEHAVIOR

The static behavior is presented in Figures 18 through 23. The parameters considered are RPM and LPO as inputs and the twist-extension coupling manifested through the twist angle at the tip, as the output. This angle will be referred as TTA (tip twist angle) in the subsequent discussion.

The TTA can be used as a measure of the twist angle ratio along the blade span. The twist angle is not a linear function of the radius but may be represented by a second degree

⁹ Pitchwise mode is a higher mode in this case and is not considered in this report.

polynomial, such that the TTA is a good parametric factor to infer the twist angle magnitude along the blade.

As mentioned before, the six models are obtained by changing the orientation of the normal vector associated to the laminate, in the three shells that constitute the spar, one at a time as shown in Figure 14.

In that figure it can be verified that Model 1 and Model 4 can be built with only one unbroken piece of laminate, wrapped around a mold. Further, one model is just the inverse of the other, in other words Model 1 is the inside out of Model 4.

The models 2 and 5 can also be considered as some sort of inverse, in a broader sense; similar reasoning may be extended to models 3 and 6.

With the above considerations, the six models can be analyzed in pairs, which is very convenient from the point of view of getting the information in a simple and concise form, so that the designer can quickly evaluate the model, keeping in view the design requirements.

The second important consequence of this inverse concept is that, Model 1 and Model 4 can supply a spectrum of twist angle requirements, for a given loading condition.

The importance of this reside in the manufacturing process, in that both models may be built by filament wound technique. This process is less expensive and more reliable

as it eliminates the filament discontinuity in the shell's junction, and requires less accurate quality control.

The convention used in the modeling process has as a aftermath that positive angles have active aerodynamic stabilizing effect, acting as a propeller governor device.

1. Models 1 and 4

Figures 18 and 24 exhibit the behavior of these two models.

The models, which were referred as inverse to each other, also show the response characteristics and behave as expected.

This may be noted by observing the displacement for a given RPM and Layer Principal Orientation Angle in Figure 26.

2. Models 2 and 5

Those models have the same inverse relationship in the TTA value. The main difference is that these two models are stiffer than the other four, as shown in Figure 17. Figure 27 shows these two models drawn together.

3. Models 3 and 6

The inverse relationship also holds here and the stiffness values are higher than that found in models 1 and 4 and lower than models 2 and 5 (Figure 17). See Figure 28 for this comparison.

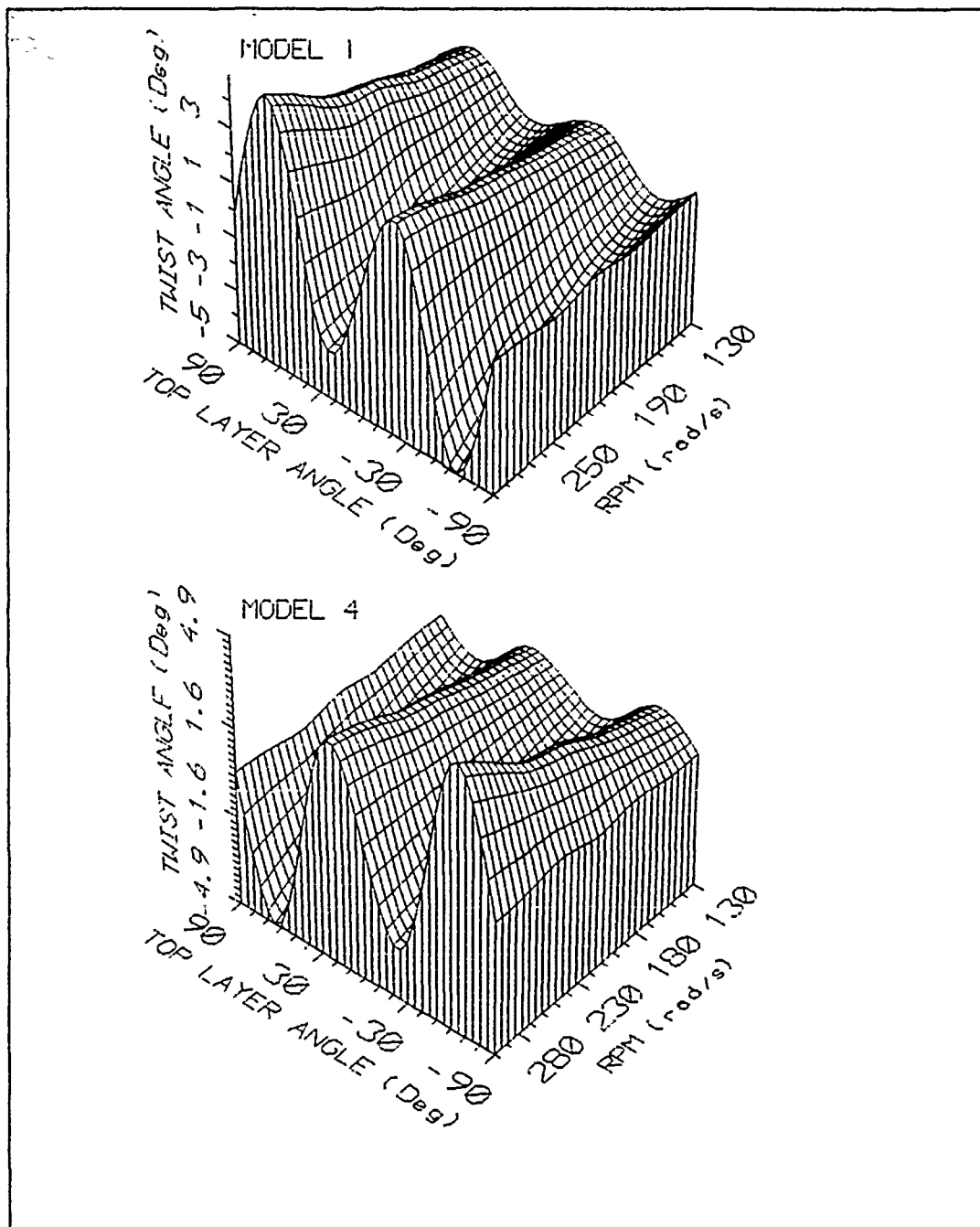


Figure 26 Models 1 and 4 static behavior comparison, inputs are RPM and Laminate Principal Orientation (LPO) angle, output is Tip Twist Angle (TTA).

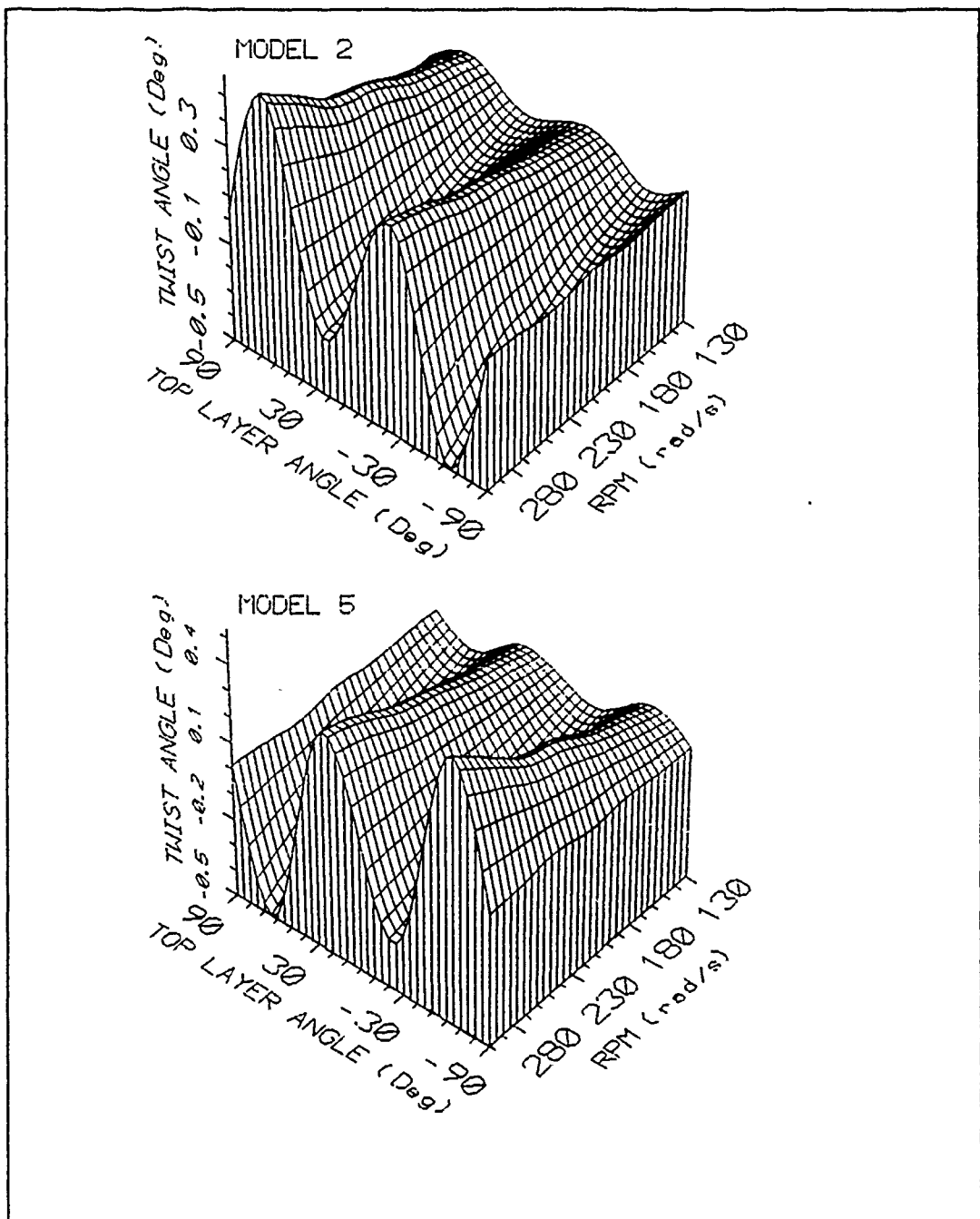


Figure 27 Models 2 and 5 static behavior comparison, inputs are RPM and Laminate Principal Orientation (LPO) angle, output is Tip Twist Angle (TTA).

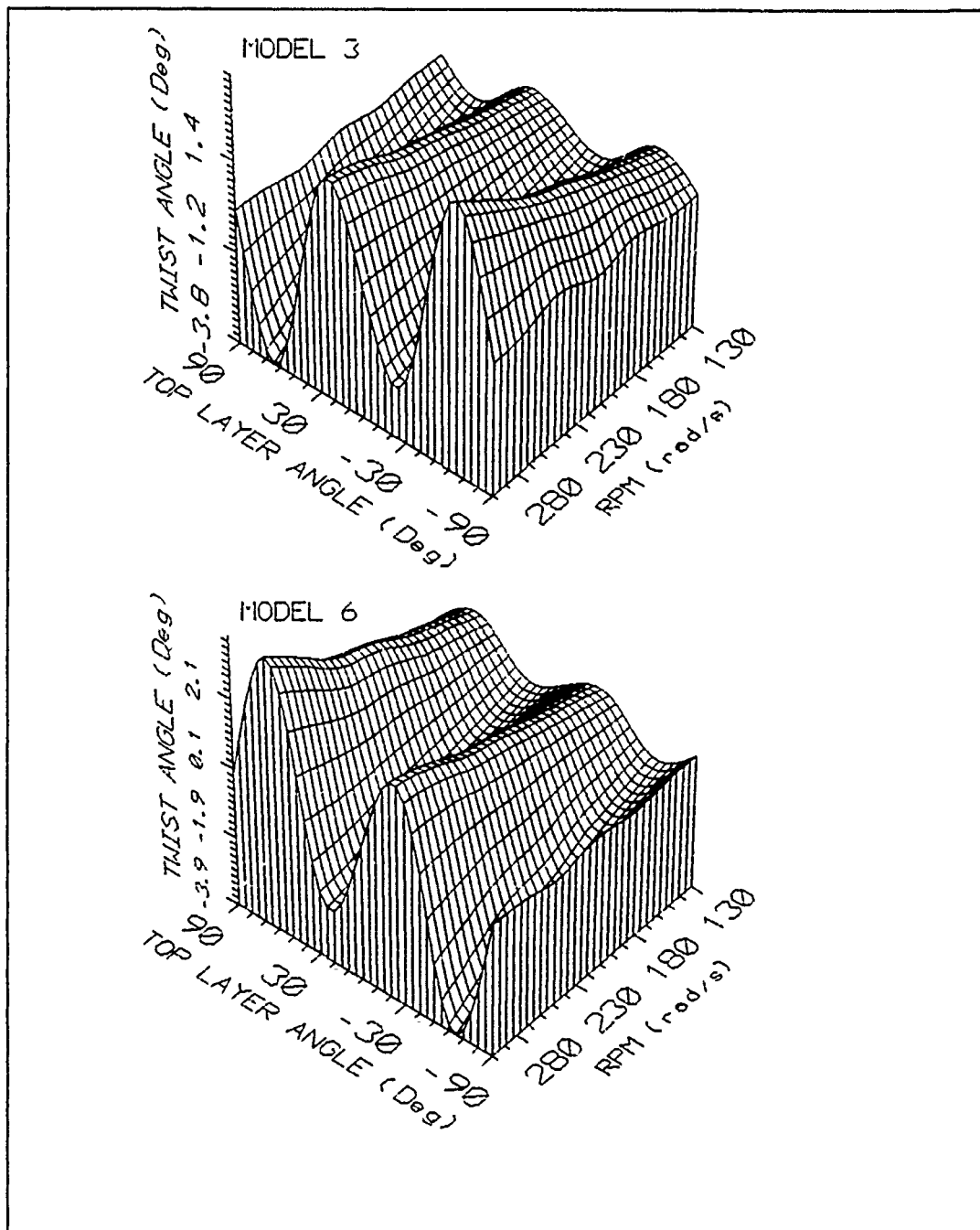


Figure 28 Models 3 and 6 static behavior comparison, inputs are RPM and Laminate Principal Orientation (LPO) angle, output is Tip Twist Angle (TTA).

VI. CONCLUSIONS AND SCOPE FOR FUTURE RESEARCH

A. CONCLUSIONS

This report presents a detailed analysis of a typical rotor blade, the focus being the static behavior in the presence of extension-twist coupling due to asymmetric stacking sequence of laminas.

Different extension-twist coupling effects are obtained, by changing the ply orientation with respect to the body axes, while keeping the stacking sequence, thickness and internal lay-up sequence as invariants.

These effects are presented in terms of carpet plots. The extension-twist coupling is measured through the angular displacement at the tip of the blade as function of RPM and Laminate Principal Orientation (LPO) angle variations.

Free vibration analysis is performed for two LPO's of the six different models. The first four fundamental frequencies show small sensitivity to these specific structural changes.

The static analysis revealed a sort of "antisymmetric" behavior within the models, allowing them to be grouped in pairs. Such behavior can be of use in the design process, to trim structural response to prescribed loads.

A structural analyst should be very careful in dealing with composite laminated structures, especially if the analyst is experienced only in structural analysis of isotropic materials. It was noted that it is very easy to be mistaken, mainly if there are asymmetries present within the laminate. It is very important to know how the local coordinates systems are established in the finite element program being used. These axes will determine the relative position of the laminate with respect to the structure. If asymmetries are present, it is possible to get different structural response and have different structural configurations, all starting with the same basic laminate.

B. SCOPE FOR FUTURE RESEARCH

Future research may be beneficial into two main areas.

The first one being to validate these models with experimental data, providing the necessary confidence in further utilization of the method envisaged.

Once the validation is done, the method can be corrected and trimmed for operational use.

Then a field that calls for attention is a dynamic characteristics mapping, that is, with the RPM and LPO as parameters obtain the fundamental frequencies as output.

This would be a 3-D composite material extension of Yntema's [1955] work for beams of isotropic material.

LIST OF REFERENCES

1. Batoz, J.L., Bathe, K.J. and Ho, L.W., 1980, A Study of Three-node Triangular Plate Bending Elements, International Journal for Numerical Methods in Engineering, Vol. 15, pp 1771-1812.
2. CASA/GIFTS, INC., 1987, Computer Aided Structural Analysis/Graphical Interactive Finite Element Total System - Users Reference and Primer Manuals, CASA/GIFTS, INC., Tucson, AZ.
3. Cook, R.D., 1981, Concepts and Applications of Finite Element Analysis, J. Wiley & Sons, New York, NY.
4. Craig, R.R. Jr., 1981, Structural Dynamics - Introduction to Computer Methods, J. Wiley & Sons, New York, NY.
5. Hodges, R.V., Nixon, M.W. and Rehfield, L.W., 1987, Comparison of Composite Rotor Blade Models: A Coupled-Beam Analysis and a MSC/NASTRAN Finite Element Model, NASA TM 89024.
6. Holt, J.H., Cases and Applications in Lotus 1-2-3 with Hal, Irwin, Homewood, IL.

7. Hoskin, B.C. and Baker, A.A., 1986, Composite Materials for Aircraft Structures, AIAA Education Series, New York, NY.
8. Johnson, W., 1980, Helicopter Theory, Princeton University Press, Princeton, NJ.
9. Jones, R.M., 1975, Mechanics of Composite Materials, Hemisphere Publishing Co., New York, N.Y.
10. Kelly, S.B., 1988, Mastering WordPerfect 5, Sybex, San Francisco, CA.
11. Kottapalli, S.B.R., 1983, Hub Loads Reduction by Modification of Blade Torsional Response, AHS 39th Annual Forum, St. Louis, MO, May.
12. Lake, R.C. and Nixon, M.W., 1988, A Preliminary Investigation of Finite Element Modeling For Composite Rotor Blades, NASA TM 100559.
13. McVeigh, A.M. and others, 1983, Aerodynamic Design of the XV-15 Advanced Composite Tilt Rotor Blade, AHS 39th Annual Forum, St. Louis, MO, May.

14. Nixon, M.W., 1987, Extension-Twist Coupling of Composite Circular Tubes Applied To Tilt Rotor Blade Design, Structural Dynamics and Material Conference, Monterey, CA, April.

15. Pritchard, J.I. and Adelman, H.M., 1988, Optimal Placement of Tuning Masses for Vibration Reduction in Helicopter Rotor Blades, NASA - Langley Research Center, February.

16. Prouty, R.W., 1986, Helicopter Performance, Stability and Control, PWS Engineering, Boston, MA.

17. Schilhansl, M.J., 1958, Bending Frequency of a Rotating Cantilever Beam. Journal of Applied Mechanics, pp 28-31, March.

18. SURFER, 1987, Reference Manual, Golden Software Inc., Golden, CO.

19. Tsai, S.W. and Pagano, N.J., 1968, Invariant Properties of Composite Materials, Composite Materials Workshop, Tsai, S.W. et al., eds., Technic Publishing Co., Stamford, CT, pp 233-253.

20. Vinson J.R. and Sierakowski, R.L., 1987, The Behavior of Structures Composed of Composite Material, Martinus Nijhoff Publishers, Dordrecht, Netherlands.

21. Wood, E.R. and Buffalano, A.C., 1965, Parametric Investigation of Aerodynamic and Aeroelastic Characteristics of Articulated and Hingeless Rotor Systems, U.S.ARMY, Trans. Research Command - Fort Eustis - VA.

22. Yntema, R.T., 1955, Simplified Procedures and Charts For The Rapid Estimation of Bending Frequencies of Rotating Beams, NACA TN 3459, Washington.

BIBLIOGRAPHIC RESEARCH

Allen, D.H., and Haisler, W.E. 1985, Introduction to Aerospace Structural Analysis, J. Wiley & Sons, New York, NY.

Astron, K.J. and Wittenmark, B., 1984, Computer Controlled Systems Theory and Design, Prentice Hall, Englewood Cliffs, NJ.

Ball, J.C. - LCDR US NAVY, 1983, XV-15 Shipboard Evaluation, AHS 39th Annual Forum, St. Louis, MO, May.

Bartley, T.M.C.H., 1983, Advanced Technology Fuselage Research Program, AHS 39th Annual Forum, St. Louis, MO, May.

*¹⁰ Batoz, J.L., Bathe, K.J. and Ho, L.W., 1980, A Study of Three-node Triangular Plate Bending Elements, International Journal of Numerical Methods in Engineering, Vol. 15, pp 1771-1812.

Blackwell, R.H., 1983, Blade Design for Reduced Helicopter Vibration, AHS Journal, Vol 28, No 3, pp 33-41.

* CASA/GIFTS, INC., 1987, Computer Aided Structural Analysis/Graphical Interactive Finite Element Total System - Users Reference and Primer Manuals, CASA/GIFTS, INC., Tucson, AZ.

Chattopadhyay, A. and Walsh, J.L., 1988, Minimum Weight Design of Rectangular/Tapered Helicopter Blades With Frequency Constraints, NASA TM 100561.

¹⁰ * means it is used as reference.

Chattopadhyay, A. and Walsh, J.L., 1988/2, Minimum Weight Design of Rotor Blades With Multiple Frequencies and Stress Constraints, NASA TM 100569.

* Cook, R.D., 1981, Concepts and Applications of Finite Element Analysis, J. Wiley & Sons, New York, NY.

Corso, J.J. and Howland, G., 1983, Contemporary Techniques for Conduct of Helicopter Airframe Fatigue Tests, AHS 39th Annual Forum, St. Louis, MO, May.

* Craig, R.R. Jr., 1981, Structural Dynamics - Introduction to Computer Methods, J. Wiley & Sons, New York, NY.

Curtiss, H.C.Jr., 1983, Modelling the Effects of Blade Torsional Flexibility in Helicopter Stability and Control, AHS 39th Annual Forum, St. Louis, MO, May.

Dokainish, M.A. and Rawtani, S., 1971, Vibration Analysis of Rotating Cantilever Plates, International Journal for Numerical Methods in Engineering, Vol. 3.

Domenic, R.E. and Hutchinson, C.K., 1983, LHX Simulation -Evaluation of a Cockpit of the Future, AHS 39th Annual Forum, St. Louis, MO, May.

Gerstenberger, W. and Wood, E.R., 1963, Analysis of Helicopter Aeroelastic Characteristics in High Speed Flight, AIAA Journal, Vol 1, No. 10, pp. 2366-2381, October.

Hanagud, S., Meyyappa M. et al., 1985, Elastic Fuselage Mode & HHC in the Coupled Rotor/Airframe Vibration Analysis, 11th European Rotorcraft Forum, p.76, September 10-13.

* Hodges, R.V., Nixon, M.W. and Rehfield, L.W., 1987, Comparison of Composite Rotor Blade Models: A Coupled-Beam Analysis and a MSC/NASTRAN Finite Element Model, NASA TM 89024.

* Holt, J.H., Cases and applications in Lotus 1-2-3 with Hal, Irwin, Homewood, IL.

* Hoskin, B.C. and Baker, A.A., 1986, Composite Materials for Aircraft Structures, AIAA Education Series, New York, N.Y.

* Johnson, W., 1980, Helicopter Theory, Princeton University Press, Princeton, NJ.

* Jones, R.M., 1975, Mechanics of Composite Materials, Hemisphere Publishing Co., New York, N.Y.

Karan, B.S., 1988, Bearingless Rotors and HHC Modeling Using RECAP, Flight Technology Methods Development-McDonnell Douglas, Mesa-AZ.

Kelly, A. and Mileiko, S.T., 1983, Handbook of Composites, Vol 4 Fabrication of Composites, Elsevier Sci. Pub. Co., Inc., New York, N.Y.

* Kelly, S.B., 1988, Mastering WordPerfect 5, Sybex, San Francisco, CA.

Kosmatka, J.B., 1989, Extension, Bending and Torsion of Anisotropic Beam With Initial Twist, in: AIAA, ASME, ASCE, AHS, and ASC, Structures, Structural Dynamics and Materials Conference, 30th, Technical Papers, pp 1799-1806 (AIAA 89-1364).

* Kottapalli, S.B.R., 1983, Hub Loads Reduction by Modification of Blade Torsional Response, AHS 39th Annual Forum, St. Louis, MO, May.

* Lake, R.C. and Nixon, M.W., 1988, A Preliminary Investigation of Finite Element Modeling For Composite Rotor Blades, NASA TM 100559.

Mase, G.E., 1970, Continuum Mechanics, McGraw-Hill, New York, NY.

* McVeigh, A.M. and others, 1983, Aerodynamic Design of the XV-15 Advanced Composite Tilt Rotor Blade, AHS 39th Annual Forum, St. Louis, MO, May.

Miller, A., 1982, Fortran Programs for Scientists and Engineers, Sybex Inc., San Francisco, CA.

NASA CP 2495, 1987, NASA/Army Rotorcraft Technology, Volume I, Aerodynamics, Dynamics and Aeroelasticity, Conference at NASA - Ames Research Center, March 17-19.

NASA CP 10007, 1983, Integrated Technology Rotor Methodology Assessment Workshop, NASA - Ames Research Center, June 21-22.

* Nixon, M.W., 1987, Extension-Twist Coupling of Composite Circular Tubes Applied To Tilt Rotor Blade Design, 28th Structures, Structural Dynamics and Material Conference, Monterey, CA, April.

Philippe, J.J. and Vuillet, A., 1983, Aerodynamic Design of Advanced Rotors With New Tip Shapes, AHS 39th Annual Forum, St. Louis, MO, May.

* Pritchard, J.I. and Adelman, H.M., 1988, Optimal Placement of Tuning Masses for Vibration Reduction in Helicopter Rotor Blades, NASA TM 100562.

Proceedings of a Workshop by NASA-Ames, 1983, Integrated Technology Rotor Methodology Assessment Workshop, NASA - Ames Research Center and U.S. Army, June 21.

* Prouty, R.W., 1986, Helicopter Performance, Stability and Control, PWS Engineering, Boston, MA.

Rehfield, L.W., Design Analysis Methodology for Composite Rotor Blades, AFWAL-TR-85-3094, U.S. Air Force, June 1985, pp. V(a).1-V(a).144.

* Schilhansl, M.J., 1958, Bending Frequency of a Rotating Cantilever Beam, Journal of Applied Mechanics, pp 28-31, March.

Sharpe, D.L., 1986, An Experimental Investigation of the Flap-Lag-Torsion Aeroelastic Stability of a Small Scale Hingeless Helicopter Rotor in Hover, NASA TR 2546, January.

Stepniewski, W.Z. and Keys, C.N., 1984, Rotary-Wing Aerodynamics, Dover Publishers Inc., New York, NY.

* SURFER, 1987, Reference Manual, Golden Software Inc., Golden, CO.

* Tsai, S.W. and Pagano, N.J., 1968, Invariant Properties of Composite Materials, Composite Materials Workshop, Tsai, S.W. et al., eds., Technic Publishing Co., Stamford, CT, pp 233-253.

* Vinson J.R. and Sierakowski, R.L., 1987, The Behavior of Structures Composed of Composite Material, Martinus Nijhoff Publishers, Dordrecht, Netherlands.

Weaver, W., and Johnston, P.R., 1895, Structural Dynamics by Finite Elements, Prentice Hall Inc., Englewood Cliffs, NJ.

Wei, F.S. and Jones, R., 1987, Dynamic Tuning of The SH-2F Composite Main Rotor Blade, AHS 43rd Annual Forum, Proceedings, Vol. 2, pp 527-537.

Wood, E.R. et al., 1985, On Developing And Flight Testing a Higher Harmonic Control System, American Helicopter Society Journal, pp. 2-20, January.

* Wood, E.R. and Buffalano, A.C., 1965, Parametric Investigation of Aerodynamic and Aeroelastic Characteristics of Articulated and Hingeless Rotor Systems, U.S.ARMV, Trans. Research Command - Fort Eustis - VA.

Wood, E.R., 1989, Notes on An Introduction to Helicopter Dynamics, Department of Aeronautical Engineering - NPS -1989.

* Yntema, R.T., 1955, Simplified Procedures and Charts For The Rapid Estimation of Bending Frequencies of Rotating Beams, NACA TN 3459, Washington.

ANNEX 1 - M120.SRC

```
$      DEFINES BLADE MODEL WITH NO ELIPSE PROJECTION
$      ( LOST 3.976 DIGITS IN DECOM )
$      ( ~ 20 MIN TO RUN 2 LDCASES )
$      NO ROOT DEFINED JUST SUPRESSED DOF OF FIRST RIB
$
```

KPOINT

```
1/.65,5.23,0
2/.455,5.23,.1103
3/0,5.23,.1545
4/-.49,5.23,.1433
5/-.49,5.23,-.1433
6/0,5.23,-.1545
7/.455,5.23,-.1103
8/.65,35.23,0
9/.455,35.23,.1103
10/0,35.23,.1545
11/-.49,35.23,.1433
12/-.49,35.23,-.1433
13/0,35.23,-.1545
14/.455,35.23,-.1103//
```

\$

\$ LINES GENERATION

\$

SLINE

```
L34/3,4,2
L45/4,5,4
L56/5,6,2
L18/1,8,21
L411/4,11,21
L512/5,12,21
L1011/10,11,2
L1112/11,12,4
L1213/12,13,2//
```

\$

\$ ARC GENERATION

\$

CARC

```
C13/1,2,3,5
C61/6,7,1,5
C810/8,9,10,5
C138/13,14,8,5//
```

\$

\$ COMPOSITE LINES GENERATION

\$

COMPLINE

```
L14/C13,L34
L51/L56,C61
L811/C810,L1011
L126/L1213,C138//
```

```

$      BLADE MATERIAL AND ELEMENTS DEFINITION (IM6/R6376)
$      BLADE MASS DISTRIBUTION = .0123 LB/IN = .00038233 SLUG/IN
$      (COMPOSITE DENSITY=.001796 SLUG/IN^3)
$      (TUNGSTEN DENSITY =.021116 SLUG/IN^3)
$      (MEAN DENSITY      =.004418 SLUG/IN^3)
$      (COMPOSITE AREA    =.086525 IN^2)
$      (COMPOSITE VOLUME =2.5957  IN^3)
$      (TUNGSTEN AREA     =.01358  IN^2 => DIA=.1315 IN)
$      (MODEL FOCUSED LENGHT=30 IN; TOTAL LENGHT=35.23 IN)
ORMAT,53
1/5.07E5,23.1E6,.338,.73E6,.004418
8.12E3,1.4E6,1.41E4//
$
$      LAYER DEFINITION [+20/-70/+20/-70/-70/+20]
$      THICKNESS = .0055 IN/LAYER * 6 = .033 IN
COMPTH
1,6/1,1,1,1,1,1
.0055,.01375,20
.0055,.00825,-70
.0055,.00275,20
.0055,-.00275,-70
.0055,-.00825,-70
.0055,-.01375,20//
$
$      ELEMENTS
$      GRIDS MUST BE GENERATED IN SAME ORIENTATION
$      STABLISH A VIEW POINT NORMAL TO SURFACE OUTSIDE (OR INSIDE)
$      WITHOUT CHANGING THIS REFERENCE GENERATE THE GRIDS FOR
$      ORTHOTROPIC MATERIALS (FILAMENT WOUNDED THINKING)
$
$      THE FIRST SIDE OF GRID DETERMINES THE REFERENCE FOR MATANG
$
GETY/TB3/1,1//
GRID4
G1/L411,L811,L18,L14
G2/L18,L128,L512,L51
G3/L512,L1112,L411,L45//
END

```

ANNEX 2 - LAYUP.AUX

FILE TO BE USED IN BUILDING THE SEVERAL LAYUPS IN
EACH M\$**.SRC FILES

\$ = LAYUP NUMBER

** = ANGLE OF TOP LAYER WITH RESPECT TO NORMAL VETOR DIRECTION

1- LAYUP GRID DEFINITION -- 6 MODELS --

M1**.SRC

GRID4

G1/L411,L811,L18,L14

G2/L18,L128,L512,L51

G3/L512,L1112,L411,L45//

M2**.SRC

GRID4

G1/L411,L811,L18,L14

G2/L512,L128,L18,L51

G3/L512,L1112,L411,L45//

M3**.SRC

GRID4

G1/L18,L811,L411,L14

G2/L512,L128,L18,L51

G3/L512,L1112,L411,L45//

M4**.SRC

GRID4

G1/L18,L811,L411,L14

G2/L512,L128,L18,L51

G3/L411,L1112,L512,L45//

M5**.SRC

GRID4

G1/L18,L811,L411,L14

G2/L18,L128,L512,L51

G3/L411,L1112,L512,L45//

M6**.SRC

GRID4

G1/L411,L811,L18,L14

G2/L18,L128,L512,L51

G3/L411,L1112,L512,L45//

2- TOP LAYER ANGLE -- 18 ANGLES --

M\$00.SRC

.0055,.01375,0
.0055,.00825,-90
.0055,.00275,0
.0055,-.00275,-90
.0055,-.00825,-90
.0055,-.01375,0//

M\$10.SRC

.0055,.01375,10
.0055,.00825,-80
.0055,.00275,10
.0055,-.00275,-80
.0055,-.00825,-80
.0055,-.01375,10//

M\$20.SRC

.0055,.01375,20
.0055,.00825,-70
.0055,.00275,20
.0055,-.00275,-70
.0055,-.00825,-70
.0055,-.01375,20//

M\$30.SRC

.0055,.01375,30
.0055,.00825,-60
.0055,.00275,30
.0055,-.00275,-60
.0055,-.00825,-60
.0055,-.01375,30//

M\$40.SRC

.0055,.01375,40
.0055,.00825,-50
.0055,.00275,40
.0055,-.00275,-50
.0055,-.00825,-50
.0055,-.01375,40//

M\$50.SRC

.0055,.01375,50
.0055,.00825,-40
.0055,.00275,50
.0055,-.00275,-40
.0055,-.00825,-40
.0055,-.01375,50//

M\$60.SRC

.0055,.01375,60
.0055,.00825,-30
.0055,.00275,60
.0055,-.00275,-30
.0055,-.00825,-30
.0055,-.01375,60//

M\$70.SRC

.0055,.01375,70
.0055,.00825,-20
.0055,.00275,70
.0055,-.00275,-20
.0055,-.00825,-20
.0055,-.01375,70//

M\$80.SRC

.0055,.01375,80
.0055,.00825,-10
.0055,.00275,80
.0055,-.00275,-10
.0055,-.00825,-10
.0055,-.01375,80//

M\$90.SRC

.0055,.01375,90
.0055,.00825,0
.0055,.00275,90
.0055,-.00275,0
.0055,-.00825,0
.0055,-.01375,90//

M\$-90.SRC

.0055,.01375,-90
.0055,.00825,0
.0055,.00275,-90
.0055,-.00275,0
.0055,-.00825,0
.0055,-.01375,-90//

M\$-80.SRC

.0055,.01375,-80
.0055,.00825,10
.0055,.00275,-80
.0055,-.00275,10
.0055,-.00825,10
.0055,-.01375,-80//

M\$-70.SRC

.0055,.01375,-70
.0055,.00825,20
.0055,.00275,-70
.0055,-.00275,20
.0055,-.00825,20
.0055,-.01375,-70//

M\$-60.SRC

.0055,.01375,-60
.0055,.00825,30
.0055,.00275,-60
.0055,-.00275,30
.0055,-.00825,30
.0055,-.01375,-60//

M\$-50.SRC

.0055,.01375,-50
.0055,.00825,40
.0055,.00275,-50
.0055,-.00275,40
.0055,-.00825,40
.0055,-.01375,-50//

M\$-40.SRC

.0055,.01375,-40
.0055,.00825,50
.0055,.00275,-40
.0055,-.00275,50
.0055,-.00825,50
.0055,-.01375,-40//

M\$-30.SRC

.0055,.01375,-30
.0055,.00825,60
.0055,.00275,-30
.0055,-.00275,60
.0055,-.00825,60
.0055,-.01375,-30//

M\$-20.SRC

.0055,.01375,-20

.0055,.00825,70

.0055,.00275,-20

.0055,-.00275,70

.0055,-.00825,70

.0055,-.01375,-20//

M\$-10.SRC

.0055,.01375,-10

.0055,.00825,80

.0055,.00275,-10

.0055,-.00275,80

.0055,-.00825,80

.0055,-.01375,-10//

INITIAL DISTRIBUTION LIST

	Nº Copies
1. Defense Technical Information Center Cameron Station Alexandria, VA 22304-6145	2
2. Library, Code 0142 Naval Postgraduate School Monterey, CA 93943-5002	2
3. Centro Técnico Aeroespacial IPD - Divisão de Aeronáutica Attn: Chefe da PAR São José dos Campos, SP BRAZIL CEP 12225	8
4. Department Chairman, Code 67 Department of Aeronautics and Astronautics Naval Postgraduate School Monterey, CA 93943-5000	1
5. Department of Aeronautics Attn: Professor Ramesh Kolar, Code 67Kj Naval Postgraduate School Monterey, CA 93943-5000	8
6. Department of Mechanical Engineering Attn: Professor Gilles Cantin, Code 69Ci Naval Postgraduate School Monterey, CA 93943-5000	1
7. Major Geraldo A. Macedo Moura Centro Técnico Aeroespacial IPD - Divisão de Aeronáutica São José dos Campos, SP BRAZIL CEP 12225	4
8. David Taylor Research Center Attn: Dr. Rem Jones, Code 1732 Bethesda, MD 20084-5000	1
9. Aeroflightdynamics Directorate Rotorcraft Dynamics Attn: Dr. Robert E. Ormiston MS 215-1, NASA AMES Moffett Field, CA 94035	1

10. NAVAIR, Code PMA 261 1
H-53/H-46 Helicopters Program Office
Attn: Program Manager
1411 Jefferson Davis Hwy, JPI,
Washington, D.C. 20361-9310
11. Department of Mathematics 1
Attn: Professor D. Danielson, Code 3Dd
Naval Postgraduate School
Monterey, CA 93943-5000